Charité – Universitätsmedizin Berlin

Campus Virchow Klinikum

Aus der Klinik für Kardiologie

DISSERTATION

Impact of colchicine on experimental Coxsackievirus B3-induced myocarditis

zur Erlangung des akademischen Grades
Doctor medicinae (Dr. med.)

vorgelegt der Medizinischen Fakultät
Charité – Universitätsmedizin Berlin

von
Jie Lin
aus Zhejiang, Volksrepublik China

Datum der Promotion: 13.12.2019

CONTENTS

Abstrakt (Deutsch)

Hintergrund

Das *nucleotide-binding oligomerization domain-like receptor pyrin domain-containing-3 (*NLRP3) Inflammasom, aktiviert die proteolytische Spaltung von pro-Interleukin (IL)-1β in seine aktive Form IL-1β und ist ein wichtiger Mediator in der Pathogenese der Coxsackievirus B3 (CVB3)-induzierten Myokarditis. Das entzündungshemmende Medikament Kolchizin, welches traditionell zur Behandlung von Gicht eingesetzt wird, übt seine Wirkung unter anderem durch die Reduzierung der NLRP3-Aktivität aus und es wurde gezeigt, dass es verschiedene Herzerkrankungen, einschließlich der Perikarditis, verbessert. Das Ziel der hier vorliegenden Arbeit war es, den Einfluss von Kolchizin auf die CVB3-induzierten Myokarditis zu evaluieren.

Methoden und Ergebnisse

In vitro wurden HL-1 Zellen mit einer Multiplikation der Infektion (m.o.i.) von 2 in serumfreien Medium (s.s) oder nur mit s.s. für 1 Stunde (h) inkubiert. Anschließend wurden die Zellen mit 100 ng/mL Kolchizin oder PBS für 4 oder 24h stimuliert, gefolgt von der durchflusszytometrischen Analyse. Es zeigte sich, dass Kolchizin den CVB3-induzierten Anteil an apoptotischen Zellen (in %) bzw. den Anteil an Coxsackievirus-Adenovirus-Rezeptor (CAR)-exprimierende Zellen um das 1,4-fache ($p<0,0001$) bzw. das 1,4-fache ($p<0,001$) senkt. Des Weiteren reduzierte Kolchizin die CVB3-induzierte NLRP3-Aktivität 4h nach der Infektion gegenüber den unbehandelten Zellen, was sich in einer 1,3-fachen ($p<0.005$), 1,2-fachen ($p=0.001$) und 2,0-fachen ($p<0.0001$) Abnahme an *apoptosis-associated speck-like protein-containing protein* (ASC)-, Caspase 1- und IL-1β-exprimierenden Zellen zeigte.

Für die *in vivo* Untersuchungen wurden C57BL6/j Mäuse an Tag 0 mit $1x10^5$ *plaque forming units* CVB3 in PBS oder PBS intraperitoneal injiziert. Vierundzwanzig h später wurden die Mäuse entweder mit 5µmol/kg Körpergewicht Kolchizin oder PBS mittels Schlundsonde behandelt. An Tag 7 erfolgte die hämodynamische Charakterisierung und anschließende Opferung der Tiere. Hierbei zeigte sich, dass Kolchizin die linksventrikuläre (LV) Funktion der CVB3-infizierten Mäuse verbesserte. Dies war mit einer 1,9-fach ($p<0.01$) und 4,6-fach ($p<0.001$) geringeren Genexpression von Col1a1 und LOX, jedoch nicht mit einer Änderung der Kollagen I/III Proteinratio, im LV der CVB3+Kolchizin Tiere gegenüber den CVB3 Tieren verbunden. Des Weiteren, verminderte Kolchizin den CVB3-vermittelten Anstieg an $CD68^+$ Monozyten in der Milz

und die Zunahmen von $CD68^+$ Monozyten im Herzen um das 1,1-fache ($p<0.01$) bzw. das 2,3-fache ($p<0.005$). Parallel dazu, war die kardiale Genexpression von Ly6C und *tumor necrosis factor* (TNF)-α in den CVB3-Tieren um das 1,4-fache ($p<0.05$) bzw. das 2,1-fache ($p<0.05$) geringer nach Applikation von Kolchizin als nach PBS. Weiterhin reduzierte Kolchizin den Anteil von ASC-, Caspase 1- und IL-1β-exprimierenden Zellen im Herzen von CVB3-infizierten Tieren.

Schlussfolgerung

Kolchizin verbesserte die LV Funktion im Model der CVB3-induzierten Myokarditis, welche die Reduzierung der NLRP3-Aktivität beinhaltet.

Abstract (English)

Background - The nucleotide-binding oligomerization domain-like receptor pyrin domain-containing-3 (NLRP3) inflammasome, activating the proteolytic cleavage from pro-IL-1β and pro-IL-18 into their active forms IL-1β and IL-18, is an important mediator in the pathogenesis of Coxsackievirus B3 (CVB3)-induced myocarditis. The anti-inflammatory drug colchicine, which is traditionally used to treat gout, exerts its effects, among others, via reducing NLRP3 activity, and has been shown to improve several cardiac diseases including pericarditis. The aim of the present study was to evaluate the potential of colchicine to improve experimental CVB3-induced myocarditis.

Methods and results - *In vitro*, HL-1 cells were infected with CVB3 at a multiplication of infection (m.o.i.) of 2 in serum starvation medium (s.s.), or incubated with s.s. for 1 hour (h). Afterwards, HL-1 cells were stimulated with 100ng/mL colchicine or PBS for 4 or 24h, followed by flow cytometry analysis. Colchicine declined the CVB3-induced percentage (%) of apoptotic cells, and the expression of the Coxsackie- and adenovirus receptor 24h post-infection, by 1.4-fold ($p<0.0001$) and 1.4-fold ($p<0.001$), respectively. Furthermore, colchicine decreased the CVB3-induced NLRP3 activity 4h post-infection, as obviated by 1.3-fold ($p<0.005$), 1.2-fold ($p=0.001$), and 2.0-fold ($p<0.0001$) lower ASC-, caspase 1-, and IL-1β-expressing cells in CVB3+colchicine versus CVB3-infected HL-1, respectively.

In vivo, C57BL6/j mice were intraperitoneally injected with $1x10^5$ plaque forming units of CVB3 or with PBS on day 0. Twenty-four h later, mice were treated with colchicine (5μmol/kg BW) or PBS via oral gavage. Mice were hemodynamically characterized at day 7 and subsequently sacrificed. Colchicine improved left ventricular (LV) function in CVB3-infected mice. This was associated with a 1.9-fold ($p<0.01$) and 4.6-fold ($p<0.001$) lower LV Col1a1 and LOX mRNA expression in CVB3+colchicine mice versus untreated CVB3-infected mice, whereas the CVB3-induced collagen I / III protein ratio was not decreased in CVB3+colchicine versus CVB3 mice. Colchicine damped the CVB3-induced % of splenic $CD68^+$ monocytes and LV presence of $CD68^+$ monocytes by 1.1-fold ($p<0.01$) and 2.3-fold ($p<0.005$), respectively, which was paralleled by 1.4-fold ($p<0.05$) and 2.1-fold ($p<0.05$) lower Ly6C and TNF-α LV mRNA expression, respectively. Colchicine further decreased the % of ASC-, caspase 1-, and IL-1β-expressing cells in the heart of CVB3-infected mice. A 4.7-fold ($p<0.01$) lower LV CVB3 mRNA expression was observed in

CVB3+colchicine versus CVB3 mice.

Conclusions - Colchicine improved cardiac function in CVB3-induced myocarditis in C57BL6/j mice, involving reduction of cardiac NLRP3 inflammasome activity.

Abbreviations

1.AB	primary antibody
2.AB	secondary antibody
ABC	avidin-biotin complex
A.dest	aqua distillate
AIM2	absent in melanoma 2
AngII	angiotensin II
ANOVA	analysis of variance
ASC	apoptosis-associated speck-like protein containing a CARD
α-SMA	alpha-smooth muscle actin
BW	body weight
BRCC3	Lys-63-specific deubiquitinase
CAR	coxsackie- and adenovirus receptor
CARD	caspase activation and recruitment domain
CCL2	(c-c motif) chemokine ligand 2
CCL7	(c-c motif) chemokine ligand 7
CCR2	(c-c motif) chemokine receptor 2
CD	cluster of differentiation
cDNA	complementary DNA
CLRs	c-type lectin receptors
CO	cardiac output
Col1	collagen I
Col3	collagen III
CTGF	connective tissue growth factor
CTLA4	cytotoxic T-lymphocyte associated protein 4
CVB3	coxsackievirus B3
Cx3Cl1	(c-x3-c motif) chemokin ligand 1 (fractalkine)
Cx3Cr1	(c-x3-c motif) chemokine receptor 1
DAF	decay-accelerating factor

DAMP	damage-associated molecular pattern
DCM	dilated cardiomyopathy
DMSO	dimethyl sulfoxide
DNA	deoxyribonucleic acid
dP/dt_{max}	maximum left ventricular pressure rise rate
dP/dt_{min}	maximum left ventricular pressure drop rate
Eam	early maturity
EAM	experimental autoimmune myocarditis
ECG	electrocardiogram
ECM	extracellular matrix
EDTA	ethylenediaminetetraacetate
EF	ejection fraction
EMB	endomyocardial biopsy
ESC	european society of cariology
EU	european union
FBS	fetal bovine serum
FOXP3	transcription factor forkhead box protein P3
GAPDH	glyceraldehydes-3-phosphate dehydrgenase
GS	goat serum
HF	heart failure
HLA	human leukocyte antigen
HLA-DQ	a cell surface receptor protein found on antigen presenting cells.
HSP	heat-shock protein
HR	heart rate
HRP	horseradish peroxidase
ICOS	inducible costimulate
IFN-β	interferon-beta
IHC	immunohistochemistry/immunohistochemical
IL	interleukin
i.p.	intraperitoneal(ly)

i.v.	intravenous(ly)
LOX	lysine oxidase
LPS	lipopolysaccharide
LV	left ventricular / left ventricle
LVP_{max}	maximum left ventricular pressure
Ly6c	lymphocyte antigen 6 complex
Mol	mole
MHC	major histocompatibility complex
MNC	mononuclear cell
MRI	magnetic resonance imaging
mRNA	messenger RNA
miRNA	micro-RNA
m.o.i	multiplication of infection
NF-kB	nuclear factor kappa-light-chain-enhancer of active B cells
NACHT	nucleotide-binding oligomerization domain
NLRP3	NOD- like receptor pyrin domain-containing-3
NLRs	nucleotide-binding oligomerization domain like receptors
NOD	nucleotide-binding oligomerization domain
ORF	open reading frame
PAMP	pattern-associated molecular pattern
PBS	phosphate-buffered saline
PCR	polymerase chain reaction
PD-1	progress death receptor 1
p.f.u	plaque forming unit
PRRs	pattern recognition receptors
PV	pression and volume
PVB19	parvovirus B19
RIG-1	rentinoic-acid-inducible gene I protein
RLRs	Rig-I-like receptors
RNA	ribonucleic acid

ROS	reactive oxygen species
RT	room temperature
SEM	standard error of the mean
SGT1	ubiquitin ligase-associated protein
SEM	standard error of the mean
s.s	starvation medium
ssRNA	single-stranded RNA
SV	stroke volume
Tau	exponential decay of LV pressure during isovolumic relaxation
TGF-β	transforming growth factor-beta
TLRs	toll-like receptors
TNF-α	tumor necrosis factor-alpha
Tregs	regulatory T cells.

1. Introduction

1.1.1 Definition

Myocarditis is a common cardiac disease, characterized by inflammation of the myocardium. Due to the various underlying etiologies, it has a wide spectrum of symptoms, ranging from mild dyspnea or chest pain to heart failure or even cardiac sudden death [1]. The term “myocarditis” was first formally proposed by Joseph Friedrich Sobernheim in 1837. Based on the definition of myocarditis at that time, myocarditis included some other cardiomyopathies such as ischemic heart disease and hypertensive heart disease. Only during the 1970s, a time when the technique of endomyocardial biopsies (EMB) in living patients became feasible, the first “modern” confirmed definition of myocarditis was proposed [2]. In 1980s, the WHO/ISFC attempted to distinguish myocarditis from other cardiomyopathies [3]. However, the exact definition of myocarditis is still under exploration. In the clinic, the diagnosis of myocarditis builds further on the combination of heart dysfunction parameters and histopathological alterations. The EMB, which allows the analysis of immune cell presence, virus type and viral copy number, is considered as the gold standard for pathological diagnosis of myocarditis. Despite the fact that the EMB is extremely important for the diagnosis of myocarditis, it is not widely executed, even in developed countries [1]. Due to the heterogeneity of clinical presentations, and no widely available specific non-invasive test, the consistency of diagnosis of myocarditis is still a challenge. In general, myocarditis is identified as a myocardial inflammatory disease with the pathological characteristic of cardiac inflammatory cell infiltration by conventional histologic and immunohistochemical (IHC) techniques. In 1986, the Dallas criteria were proposed and established a histopathological standard for the diagnosis of myocarditis [4]. The Dallas criteria and classifications, which depend on conventional histopathological methods, have been used for more than three decades, even though there were some reservations from both objective and subjective sources, including the variation in pathologist interpretation, and variance with other markers of viral infection and immune activation in the heart. Due to the availability of molecular biological analyses and revelation of new mechanisms of myocarditis, Dallas criteria have been considered to be not sensitive enough for the accurate diagnosis of myocarditis [1, 5]. Based on the knowledge of inflammatory cell presence in the heart of myocarditis patients and animal experimental models, IHC criteria of myocarditis have been discussed and established. Caforio and colleagues [1]

defined myocarditis as a cardiac disorder with the following IHC criteria: exhibit ≥14 lymphocytes/mm^2 including ≤4 monocytes/mm^2, with the presence of $CD3^+$ T lymphocytes ≥7 cells/mm^2. The development of new molecular techniques including polymerase chain reaction, miRNA profiling, and *in situ* hybridization, may definitely raise the sensitivity of diagnosis of myocarditis.

1.1.2. Epidemiology

The exact incidence and prevalence of myocarditis is unconfirmed, but likely much underestimated, due to lack of unanimous criteria for myocarditis diagnosis and different diagnosis standards of myocarditis. Karjalainen *et al.* [6] reported that the incidence of acute myocarditis in young men was approximately 0.17% per year. In this case, the annual incidence of myocarditis was estimated via electrocardiographic (ECG) changes, clinical symptoms, and cardiac enzyme elevation, mostly without EMB analysis. Moreover, fatal myocarditis often manifests as sudden death, most common in infants and young adults. The proportion of myocarditis-caused sudden death was about 10% in young soldiers, and the incidence was around 0.002% per year [7]. Another study revealed via autopsy analysis that myocarditis made up 8.6% of all adult sudden death [6]. Data from clinical trials likely severely underestimate the incidence of myocarditis, because the majority of myocarditis presentation is subclinical, from which patients recover spontaneously without any specific treatment.

1.1.3. Etiology

According to the cause of inflammation, including infections, drugs, toxic substances, and autoimmune diseases, myocarditis can be classified into microbial and non-microbial [1, 8] (**Table 1**). Viral infection is the most common cause of myocarditis. Based on EMB evaluations and new advanced techniques for detecting pathogens, it was suggested that the most common viral causes of myocarditis were enteroviruses, particularly coxsackievirus B3 (CVB3) [9], adenovirus [10], parvovirus B19 (PVB19) [11], human herpesvirus-6 [12], Epstein-Barr-virus [13], cytomegalovirus [14], hepatitis C virus [15], human immune deficiency virus [16] and influenza viruses [17], varying from different regions. The data of EMB assays from the 1980s to 1990s showed that CVB3 infection was the most common identified cause of myocarditis [18, 19].

Table 1. Infectious myocarditis [1]

Infectious myocarditis	
Viral	RNA viruses: Coxsackieviruses A and B, Echoviruses, Polioviruses, Influenza A and B viruses, Respiratory syncytial virus, Mumps virus, Measles virus, Rubella virus, Hepatitis C virus, Dengue virus, Yellow fever virus, Chikungunya virus, Junin virus, Lassa fever virus, Rabies virus, Human immunodeficiency virus-1
Bacterial	*Staphylococcus, Streptococcus, Pneumococcus, Meningococcus, Gonococcus, Salmonella, Corynebacterium diphtheriae, Haemophilus influenzae, Mycobacterium (tuberculosis), Mycoplasma pneumoniae, Brucella*
Fungal	*Aspergillus, Actinomyces, Blastomyces, Candida, Coccidioides, Cryptococcus, Histoplasma, Mucormycoses, Nocardia, Sporothrix*
Parasitic	*Trichinella spiralis, Echinococcus granulosus, Taenia solium*
Protozoal	*Trypanosoma cruzi, Toxoplasma gondii, Entamoeba, Leishmania*
Rickettsial	*Coxiella burnetii (Q fever), R. rickettsii (Rocky Mountain spotted fever), R. tsutsugamuschi*
Spirochaetal	*Borrelia (Lyme disease), Leptospira (Weil disease)*

Nevertheless, a landmark study by Kühl *et al.* in 2005 [20] reported that the prevalence of parvoviruses was much higher than enteroviruses in adult idiopathic dilated cardiomyopathy (DCM). The data showed that 9.4%, 4.2%, and 51.4% were enterovirus-, adenovirus-, and PVB19-positive, respectively, and 27.3% of viral genome-positive cases were dual or multiple viral infections [21], indicating a shift in cardiotropic viruses over the years. Furthermore, Bowles *et al.* [10] indicated that adenovirus, enterovirus, and cytomegalovirus were the most common

three categories of viruses in viral infected-induced myocarditis. The Keshan disease is a type of specific myocarditis, which is prevalent in a specific region, and at a specific period [22], and some myocarditis cases occur in particular patients under specific disease conditions such as sepsis or immune deficiency [1].

1.1.4. Pathology and prognosis

Myocarditis is defined as a myocardial inflammation by which the inflammatory response determines the prognosis of myocarditis. Regardless of its etiology, the inflammatory response axis develops from an acute inflammatory stage to a subacute and chronic inflammatory stage, followed by a cardiac remodeling stage with myocardial fibrosis and cardiac dysfunction. The Dallas classification, which depends on conventional histological staining (hematoxylin-eosin), has been applied for myocarditis pathologic diagnosis for decades, and is not as sensitive as new techniques used today [1]. Based on immunopathology findings, myocarditis is classified as acute lymphocytic myocarditis, chronic lymphocytic myocarditis, giant cell myocarditis, sarcoidosis myocarditis, and eosinophilic myocarditis. Depending on the infiltrated inflammatory cells, alterations of the myocardial structural and pathogenic evaluations, the process of viral myocarditis is divided into four phases: pre-infection phase, phase I, phase II and phase III. Phase I to III correspond to acute myocarditis, chronic myocarditis, and cardiac remodeling stage, respectively [1] (**Figure 1**). The outcome of viral myocarditis is extremely polarized: on the one hand, the majority of myocarditis can be spontaneously cured without specific treatment; on the other hand, a few infected individuals develop myocarditis to devastating ends and even sudden death. Biopsy-proven chronic myocarditis can progress to DCM associated with a poor prognosis [23]. Biopsy histological assays of dilated cardiomyopathy showed the rates of inflammatory disorder (myocarditis) were 30-40% and 46% in adults and in children under 18 years old, respectively [24]. Moreover, some of the myocarditis cases would rapidly develop to sudden death, and its exact incidence is unclear. Several studies investigating cardiac sudden death in youth demonstrated that 2-42% of cases were related to myocarditis [2, 25, 26]. This explicit difference between the outcomes of myocarditis might be associated with genomic and environmental factors. However, which exact genes determine the susceptibility of viral

myocarditis is still unclear. In mice, studies demonstrated that some non-major histocompatibility complex (non-MHC) immunoregulatory genes such as Eam1, Eam2, CTLA4, ICOS and PD-1 may have a greater impact than MHC genes on susceptibility [21, 27].

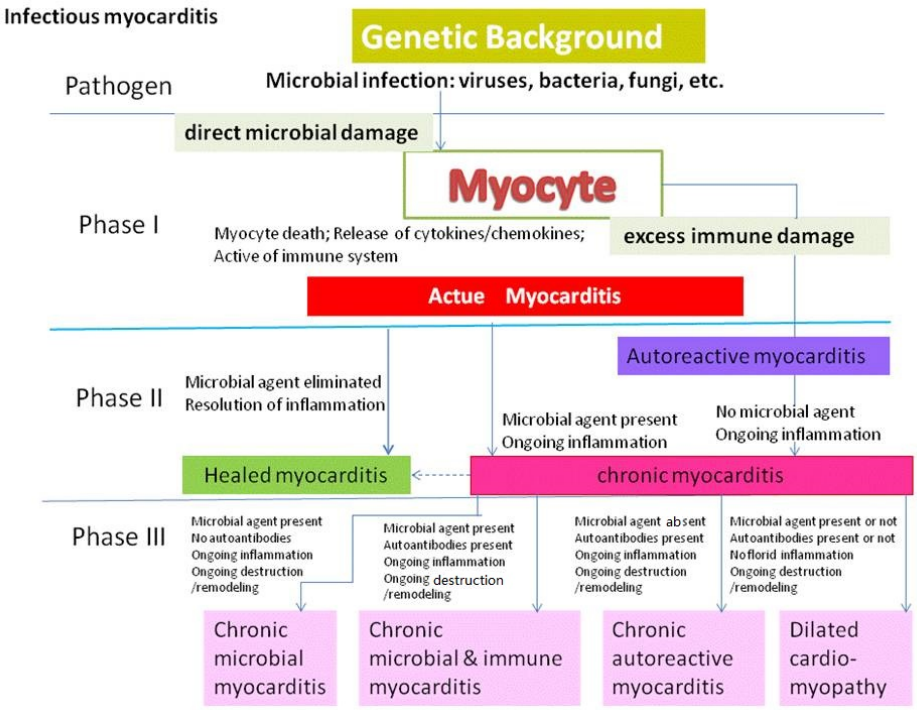

Figure 1. Course of Infectious myocarditis [1]. The Phase I-III is not the defined process, depending on the pathological and molecular detection of the heart.

1.2. Animal model of myocarditis

1.2.1. Coxsackievirus B3-induced viral myocarditis mouse model

The myocarditis experimental animal model has successfully been set up in a variety of species, but the most used animal is the mouse. The CVB3-induced mouse myocarditis model is considered as acute lymphocytic myocarditis, which is characterized by T lymphocyte infiltration, and a pathogenesis similar to human [28, 29]. Furthermore, the mouse myocarditis model has plenty of advantages compared to other species models for myocarditis research. For example, the availability of transgenic strains, and sensitivity of mice for cardiotropic viruses, is convenient to explore the role of a specific gene in the disease process, and enables the discovery of distinct mechanisms underlying myocarditis. Viral genome analysis from biopsies and autopsies demonstrated that CVB3 was one of the most common viruses causing myocarditis. In the 1970s, the CVB3-induced myocarditis mouse model was established with histological lesions similar to

human myocarditis pathological alterations. Until today, the CVB3 model has been the most widely used mouse model in myocarditis research [29, 30]. The cellular and molecular mechanisms of CVB3-infected hearts have mostly been investigated in murine models [21, 30]. The outcome of viral myocarditis depends on the contribution of the viruses as well as the individual susceptibility, which is mainly based on the immune system. Different susceptibility of mouse strains to CVB3 infection leads to a dramatic variety in the prognosis of CVB3-induced myocarditis. The immunocompetent mouse strain C57BL/6 is susceptible to develop into an acute, but not chronic myocarditis. Conversely, C3H/He, BALB/c and NMRI are susceptible to develop into chronic myocarditis and dilated cardiomyopathy [27, 31-35]. Even in the same strain of inbred mice, different experimental circumstances might lead to inconsistent reactions to CVB3 infection [36]. Both sexual hormones have effects on the myocarditis process. Male mice are more susceptible to CVB3-induced myocarditis, and have a more severe inflammatory response compared to female mice [37]. Currently, the three mostly used myocarditis mouse models are the following [38]:

(1) CVB3-only model: mice are infected via intraperitoneal injection (i.p.) with purified virus or RNA from various CVB3 strains after passage through HeLa cells;

(2) Hybrid-CVB3 model: mice are i.p. inoculated with CVB3 originally isolated from a patient and passaged through Vero cells;

(3) Experimental Autoimmune Myocarditis (EAM): EAM is induced by cardiac myosin/cardiac peptides and adjuvants via vein injection (i.v.).

1.2.2. Phases of Coxsackievirus B3-induced myocarditis in the mouse model

The CVB3 infectious process can be divided into four phases: the pre-infection phase (phase 0) outlines the susceptibility to viral infection, whereas phase I to III are after virus transmission into myocytes [21]. This classification depends on histopathologic and molecular assessment. Phase 0: this phase means susceptibility to viral myocarditis at pre-infection. The exact mechanisms of susceptibility to viral infection of the heart and subsequent reaction are still not fully clear. Based on mice studies, some immune-related genes (MHC and non-MHC), sexual hormones, nutrients, and habitat environment affect the susceptibility to viral myocarditis [31, 35, 39, 40].

Phase I: this is the most crucial phase of viral myocarditis, from the initial invasion of the virus

into cardiomyocytes to complete viral elimination. Although it is still difficult to depict the specific pathogenesis of viral myocarditis, a number of molecular mechanisms have been identified including the entry of the virus into the myocyte, the reaction of innate immunity against viral replication and virus clearance, and transmission of virions to adjacent cells [41-44]. The early myocardial injury occurs at phase I, which mainly comprises direct virus-induced damage, followed by inflammatory and immune responses during the processes.

Phase II: after the infectious virus is eliminated by the host immune system, the persistence of the viral genome is maintained for an extensive period in the myocardium.

Phase III: cardiac remodeling in the absence of infectious virus, with or without the viral genome.

1.2.3. Characteristics of Coxsackievirus B3

Coxsackievirus was first named in 1947 by Dalldorf and Sickles, who divided Cosackieviruses into subsets A (23 serotypes) and B (6 serotypes) [45]. CVB3 is one serotype of the B subset and is a type of cardiotropic virus with a single positive-strand RNA. SH and CG are the most virulent strains in the four variants of CVB3 (CG, SH, ST or NR), which can induce diverse pathological phenotypes of viral myocarditis within various mouse strains (C57BL/6, B10.D2, BALB/c, DBA/2, A/J or C3H/HeJ) [35]. The virion of CVB3 is a non-enveloped icosahedral particle of approximately 30 nm diameter, containing an outside protein capsid and internal viral genome. The protein capsid is composed of 4 proteins: VP1, VP2, and VP3 (construct outer layer) and VP4 (on the internal side). The linear ssRNA genome of approximately 7.5 kb comprises an open reading frame (ORF), flanked on both 3’ and 5’ termini with untranslated regions (UTRs). The ORF contains genes encoding for 11 proteins involved in viral replication [36] (**Table 2**).

Table 2. Coxsackievirus B3-associated viral proteins and their function [36]

Functions	Proteins
capsid proteins	VP1, VP2, VP3 and VP4
viral proteases	2A and 3C
RNA-dependent-RNA-polymerase	3D
proteins involved in RNA synthesis	2B and 2C
a primer of initiation of RNA synthesis	3AB
a small polypeptide (VPg)	3B

1.2.4. Coxsackievirus B3 replication lifecycle

Replication of CVB3 mainly depends on the host cell because it is a kind of cell parasite. There are several mechanisms involved in virus attachment to the target cell, including attachment to the major Coxsackie- and adenovirus receptor (CAR) and co-receptor, decay-accelerating factor (DAF). CAR is a receptor for coxsackie- and adenoviruses and is expressed in various cells such as epithelial and endothelial cells, and cardiomyocytes [46]. DAF, also known as CD55, not only regulates the complement system, but also acts as a co-receptor to couple coxsackie- and other enteroviruses on the cell surface [47, 48]. Cardiomyocytes express both CAR and DAF on their surface. The CVB3 life cycle begins by binding and clustering to DAF, which moves the virus to the main receptor (CAR), which allows internalization of the virus into the myocyte; afterwards, the internalized virion genome replicates (+ss-RNA) and assembles with translated scaffold proteins to form new progenies; finally, virion progenies are released toward adjacent cells [36] (**Figure 2**). The expression of CAR and DAF play an important role in the susceptibility of the myocyte to CVB3. Previous studies have demonstrated that the heart and exocrine pancreas are the most vulnerable organs to the CVB3. Nevertheless, the expression of CAR and DAF is only at a moderate level in cardiomyocytes [49, 50]. Since CAR and DAF are only modestly expressed on cardiomyocytes [51, 52], other unknown mechanisms for CVB3 attachment and entering into the target cell may be suggested.

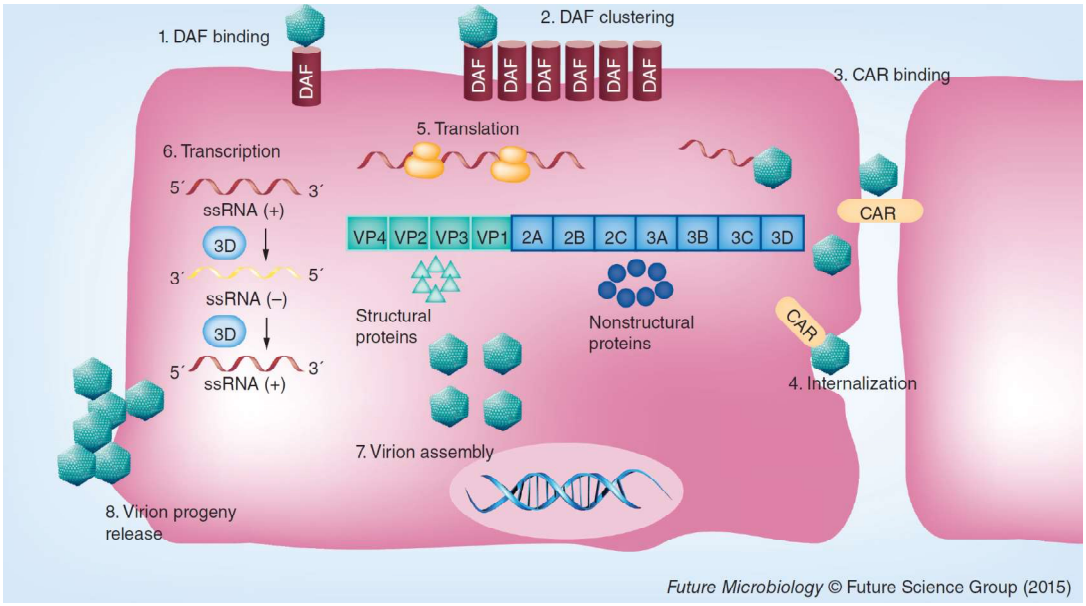

Figure 2. Coxsackievirus B3 life cycle [36]. A complete CVB3 life cycle in the myocardium is outlined from step 1 to step 8, and is generally defined by three parts: firstly, the CVB3 life cycle begins with CVB3 DAF binding, followed by DAF clustering, CAR binding, CVB3-CAR complexity internalization, and successful CVB3 entering into the cell. Secondly, CVB3 replication takes place in the host cell, including translation, transcription, and virion assembly. Finally, the entire assembled CVB3 is released out of the host cell to infect adjacent cells.

1.3. Cell damage and immune response

1.3.1. Host cell injury

Numerous studies demonstrate that CVB3-induced acute myocarditis leads to myocardium destruction including direct viral-mediated effects and consequent aberrant immune and inflammatory responses. Furthermore, there is accumulating evidence that the inflammatory response is the main trigger of cardiac dysfunction rather than the direct CVB3-induced damage [53]. CVB3-induced direct damage of the host cells mainly comprises inhibition of cardiomyocyte DNA transcription and mRNA translation, and cell structure disruption due to viral proteases, which cleave structural proteins. The subsequent release of molecules induces the innate and adaptive immune response [40, 54]. Recent experimental studies have partly revealed the molecular mechanisms of immunological responses, which lead to persistent injury of cardiomyocytes, independent of direct virus-induced viral damage [55].

1.3.2. Innate immunity and the NLRP3 inflammasome

The maintenance of organism homeostasis is a primary function of the innate immune system.

Pattern recognition receptors (PRRs) play a key role in the innate immune response recognizing damage-associated molecular patterns (DAMPs) and pathogen-associated molecular patterns (PAMPs), which are unique to each pathogen. Based on their location, PRRs can be classified as membrane-bound PRRs and cytoplasmic PRRs. Four well-known PRRs are Toll-like-receptors (TLRs), C-type lectin receptors (CLRs), Rig-I-like receptors (RLRs) and nucleotide-binding oligomerization domain like receptors (NLRs) [56]. PRRs can recognize PAMPs like lipopolysaccharide (LPS) of Gram-negative organisms, zymosans of yeast, glycolipids of mycobacterium, and single or double-stranded RNA viruses. Recently, studies have indicated that cardiac PRRs can also recognize endogenous materials released from dying or injury host cells [57]. A report indicated that levels of TLR1, TLR2, TLR3, TLR4, TLR6, TLR7, TLR8, TLR9, TLR13, RIG-I, MDA5 and LGP2 were significantly upregulated in the heart of CVB3-induced myocarditis compared to uninfected control mice [58]. Several animal studies, including our prior studies, have consistently demonstrated that TLR4 [59], TLR9 [60], and NOD2 [61] are associated with the susceptibility of viral myocarditis. Knockout of these different genes can attenuate the viral-induced heart injury and viral load. Besides PRRs, inflammasomes also play a crucial role in the innate immune system. Inflammasomes are a group of cytosolic protein complexes that are formed to mediate host immune responses to microbial infection and cellular damage. Several inflammasomes have been described including the NLRP and absent in melanoma 2 (AIM2) families, containing a NLR domain and pyrin, and HIN domain-containing protein (PYHIN) domain, respectively [62]. The NLRP3 inflammasome is the most thoroughly described inflammasome complex to date, and is involved in the microbial and sterile inflammatory response. The common characteristic of the NLRP3 molecular structure is a N-terminal pyrin domain (PYD), central nucleotide-binding oligomerization domain (NACHT), followed by a leucine-rich repeat domain (LRR) at the C-terminus [63]. The NLRP3 inflammasome complex contains NLRP3, an adaptor protein apoptosis-associated speck-like protein containing a CARD domain (ASC), and the cysteine protease caspase 1. Assembly of the inflammasome leads to autocatalysis and activation of caspase 1, which subsequently converts pro-IL-1β and pro-IL-18 into their mature form IL-1 and IL-18 (**Figure 3**). These secreted cytokines initiate an inflammatory cascade including the recruitment of innate immune cells and further adaptive immune responses [64]. Abundant ligands including endogenous and

exogenous molecules can trigger the formation of the NLRP3 complex. Most of them activating NLRP3 are not via direct coupling. In general, formation of a functional NLRP3 complex is a two-step model consisting of priming and activation [62]. Generally, the priming process comprises the upregulation of transcription and post-translation modification. Priming stimuli bind any receptors whose signaling leads to the activation of the transcription factor NF-κB, followed by the upregulation of the transcription of both IL-1β and NLRP3 [65, 66]. These comprise ligands for IL-1R1, TLRs and NLRs. The priming signaling stimulates NLRP3 deubiquitination of its LRR domain, which is mediated by Lys-63-specific deubiquitinase (BRCC3), leading to the oligomerization of NLRP3 [67]. Furthermore, under the priming condition, the heat-shock protein 90 (HSP90) and the ubiquitin ligase-associated protein SGT1 dissociate from the NACHT and LRR domains, allowing NLRP3 to adopt a conformation that enables the interaction with other inflammasome components such ASC and caspase 1 [68]. A functional inflammasome NLRP3 is triggered by simultaneous provision of both priming and activation signaling (**Figure 3**). The activation step of the NLRP3 inflammasome involves various agonists including exogenous and endogenous activators that trigger the specific formation of the NLRP3 inflammasome complex and finally activation of caspase 1. However, the precise mechanism of inflammasome NLRP3 activation is still obscure. Several studies have shown that potassium efflux [69], calcium influx [70], and mitochondrial-associated activators [71] can activate NLRP3 inflammasome. The NLRP3 inflammasome plays a key role in myocarditis, supported by experimental studies showing the cardiac benefit via blocking the NLRP3 inflammasome [72]. Our center reported that CVB3-induced myocarditis significantly increased the expression of NOD2 and NLRP3 in the heart of CVB3-infected mice compared to uninfected control mice. NOD2 knockout were protected against myocarditis through downregulation of NLRP3 expression [61].

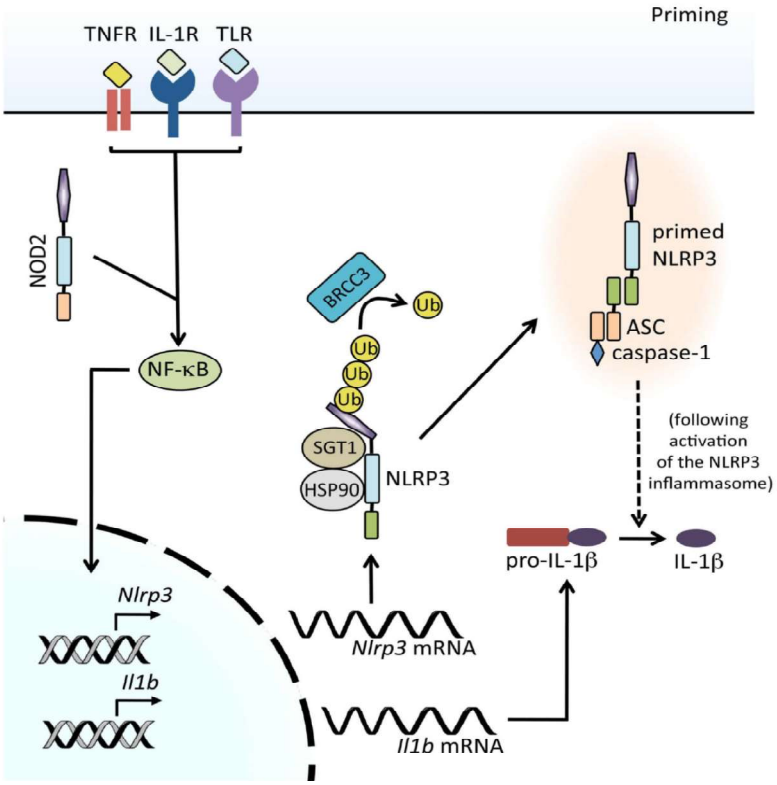

Figure 3. NLRP3 inflammasome priming [62, 73]. Formation of the NLRP3 inflammasome complex requires simultaneous NLRP3 priming and activation. NLRP3 priming mainly involves the NF-κB pathway, which increases the transcription of NLRP3, and includes NLRP3 deubiquitinase for NLRP3 complex assembly.

1.4. Colchicine

1.4.1. Safety of colchicine

Colchicine, an ancient drug, has been documented as a treatment option for gout for more than a thousand years. The long history of its medical use indicates the safety of colchicine. Surprisingly, the Food and Drug Administration (FDA) only approved colchicine in 2009, as a new drug for Familial Mediterranean fever and acute gout. In general, the medical safety of colchicine is high. However, colchicine has a few serious side-effects, which can be reversed after its withdrawal [74]. Gastrointestinal intolerance is one the most common side-effects. Based on colchicine's safety and anti-inflammatory features, colchicine is suggested as a potential novel adjunct treatment option within oncology, immunology, cardiology, and dermatology of inflammatory disease [75, 76].

1.4.2. Colchicine and cardiac disease

Solomon *et al.* [77] reported that colchicine users had a 49% lower risk of primary cardiovascular events and a 73% reduction in all-cause mortality than non-colchicine using patients with gout. A few other cohort trials indicated that colchicine may lower cardiovascular events in various cardiovascular diseases, including chronic heart failure,coronary heart disease, and pericardiotomy, compared with control patients, but the definite mechanisms are not yet explored [74, 78, 79].

1.4.3. The main anti-inflammatory mechanism of colchicine

Colchicine is a tubulin-binding drug, which binds to soluble tubulin to form a tubulin-colchicine complex. This complex inhibits microtubule dynamics and affects cellular function. The main pharmacologic mechanism underlying the anti-inflammatory effects of colchicine is related to the assembly of tubulins, which causes disruption of microtubule formation and inhibition of inflammatory cells' functions including the release of cytokines and chemokines. However, the exact accurate mechanisms are still obscure [75, 80]. Microtubules are related to many elementary cellular processes, including mechanical support, organization of the cytoplasm, transport, motility, and mitosis [81].

2. Objectives

Nuki *et al.* [80] investigated the pathophysiology of crystal-induced inflammation, offering new insights into the mechanism of action of colchicine's anti-inflammatory properties, including inhibition of the NLRP3 inflammasome and subsequent interleukin 1β (IL-1β) processing. Another study demonstrated that colchicine decreased NLRP3 inflammasome-mediated inflammation and improved obesity-related metabolic dysregulation [82]. Moreover, a clinical case report showed that early low-dose colchicine therapy as an adjunct to conventional therapy led to a great clinical improvement in an Epstein-Barr virus and Cytomegalovirus-induced myocarditis patient [83]. The 2015 ESC pericarditis guidelines recommend colchicine as a first-line treatment for acute pericarditis, by which viral infection is the most common etiology in developed countries [76, 84]. Whereas the therapeutic effect of colchicine for sterile inflammation is widely accepted, the ESC guidelines (2015) for the treatment of pericarditis and a few clinical case reports further support colchicine as having possible beneficial effects in virus-induced inflammation. The high safety and low cost of colchicine make it easily available in clinical practice. In view of its potential clinical application in myocarditis patients, this study aimed to answer the following questions:

(1) Can colchicine bring any benefits in experimental CVB3-induced myocarditis?

(2) Do the colchicine-mediated protective effects in experimental CVB3-induced myocarditis involve modulation of the NLRP3 inflammasome?

3. Materials and methods

3.1. Materials (Detailed on Tables 3 to 10)

Table 3. Consumption materials

Article	Description	Company
96-well plate	Multiply®-PCR	Sarstedt, Nürnbrecht, Germany
Cell strainer	70 µm	BD Biosciences, San Jose, CA, USA
Cover slides	21x26 mm	R.Langenbrinck, Mendingen, Germany
Cryotubes	1.5 mL	Carl Roth, Karlsruhe, Germany
Falcon tubes	15 mL, 50 mL	Corning, New York, NY, USA
Gloves	Various Sizes	Sempercare, Northamptonshire, United Kingdom
Masks		Charité, Berlin, Germany
Microtome blades	A35 type	Feather, Cologne, Germany
PCR-tube with conical lid	0.2 mL	Biozym, Hess. Oldendorf, Germany
Pipette tips	10-1000 µL	Biozym, Hess. Oldendorf, Germany
Transfer pipettes	10, 25, 50 mL	Biozym, Hess. Oldendorf, Germany
Plastic cannulas	18G und 20G	B. Braun, Melsungen,

		Germany
Reaction tubes	Safe-Lock or RNAse-free	Sarstedt, Nürnbrecht, Germany
Scalpels	Cutting tool	Feather, Cologne, Germany
Slides	SuperFrost™ Plus	R.Langenbrinck, Emmendingen, Germany

Table 4. Laboratory equipment

Equipment	Description	Company
Conductance catheter	1.2 French	Scisense Inc., Ontario, Canada
Cryostat	CryoStar™ NX70 Cryostat	Thermo Fisher Scientific, Waltham, MA, USA
Flow cytometry	MACSQuant Tyto	Miltenyi Biotec, Bergisch Gladbach, Germany
Freezer -20	Economic super	Bosch AG, Stuttgart, Germany
Freezer -80	Nuaire Ultralow Freezer	Zapf Instrumente, Sarstedt, Germany
Dissociator	gentleMACS Octo	Miltenyi Biotec, Bergisch Gladbach, Germany
Homogenizer	T25 digital ULTRA-TURRAX®	IKA, Staufen, Germany
Horizontal shaker	Promax 1020	Heidolph, Schwabach, Germany
Ice maker	AF-10	Scotsman, Vernon Hills, IL, USA
Incubator	Function Line	Heraeus, Osterode, Germany
Microscope	DM2000LED	Leica, Bensheim, Germany
pH meter	Knick Digital 646	Beyer, Düsseldorf, Germany
Photometer	SPECTRA max	Molecular Devices, Biberach an der Riß, Germany
Pipettes	Single and multi-channel	Eppendorf, Wesseling-Berzdorf, Germany
Pressure-volume amplifier system	MPVS 300/400	Millar Instruments, Houston, TE, USA
Spectrophotometer	NanoDrop 1000	Thermo Scientific PEQLAB,

		Erlangen, Germany
Thermocycler	Mastercycler	Eppendorf, Wesseling-Berzdorf, Germany
Thermomixer	Comform	Eppendorf, Wesseling-Berzdorf, Germany
Tabletop centrifuge	Centrifuge 5415R	Eppendorf, Wesseling-Berzdorf, Germany
Ventilator	Mini-Vent	Harvard Apparatus,Holliston, MA, USA
Vortex mixer	NeoLab 7-2020	IKA-Labortechnik, Staufen, Germany

Table 5. Buffer, reagents and kits

Article	Company
1% β-Mercaptoethanol	Sigma-Aldrich Chemie GmbH, Taufkirchen, Germany
3-Amino-9-ethylcarbazole (AEC)	Sigma-Aldrich Chemie GmbH, Taufkirchen, Germany
ABC Blocking Kit	Vector Labs, Burlingame, KA, USA
ABC Kit Standard	Vector Labs, Burlingame, KA, USA
Acetic acid (96-100%)	Carl Roth, Karlsruhe, Germany
Acetone	VWR International GmbH, Darmstadt, Germany
Bovine serum albumin (BSA)	Carl Roth, Karlsruhe, Germany
Calcium chloride	VWR International GmbH, Darmstadt, Germany
Di-Sodium hydrogen phosphate dihydrate	Merck Millipore, Darmstadt, Germany
Distilled water	Alleman Pharma GmbH, Rimbach, Germany
DNAse I	Qiagen, Hilden, Germany
EnVision	Dako, Hamburg, Germany
Ethylenediaminetetraacetate (EDTA)	VWR International GmbH, Darmstadt, Germany
Ethanol	Sigma-Aldrich Chemie GmbH,

	Taufkirchen, Germany
Fetal Bovine Serum (FBS)	Biochrom, Berlin, Germany
Fixation/Permeabilization kit	BD Bioscience, Heidelberg, Germany
Formalin	Sigma-Aldrich Chemie, Taufkirchen, Germany
Goat Serum	Sigma-Aldrich Chemie, Taufkirchen, Germany
High Capacity cDNA Reverse Transcription Kit	Applied Biosystems, Darmstadt, Germany
Hydrogen peroxide solution (H_2O_2)	Merck, Millipore, Darmstadt, Germany
Isopropanol	Sigma-Aldrich Chemie, Taufkirchen, Germany
Kaiser's glycerol gelatin	Carl Roth, Karlsruhe Germany
Magnesium chloride	VWR International GmbH, Darmstadt, Germany
Mayer’s hemalum solution	Merck Millipore, Darmstadt, Germany
Neonatal Heart Dissociation Kit	Miltenyi Biotec, Bergisch Gladbach, Germany
N, N-dimethylformamide	Carl Roth, Karlsruhe, Germany
Potassium chloride (KCl)	Merck Millipore, Darmstadt, Germany
Potassium dihydrogen phosphate (KH_2PO_4)	Merck Millipore, Darmstadt, Germany
RNase-free water	Thermo Fisher Scientific, Waltham, MA, USA

Sodium acetate (CH_3COONa)	Merck Millipore, Darmstadt, Germany
Sodium chloride (NaCl)	Applichem, Darmstadt, Germany
Sodium hydrogen phosphate (Na_2HPO_4)	Merck Millipore, Darmstadt, Germany
Tissue-Tek OCT	Sakura, Zoeterwoude, Netherlands
Trizma Base	Calbiochem/Merck Millipore, Darmstadt, Germany
Trizma HCl	Carl Roth, Karlsruhe, Germany
TRIzol	Thermo Fisher Scientific, Waltham, MA, USA

Table 6. Real-time PCR reagents

Reagents	Company
Optical 384-well reaction Plate	Applied Biosystems, Darmstadt, Germany
Optical Adhesive film	Applied Biosystems, Darmstadt, Germany
TaqMan Gene expression Master Mix (2×)	BD Bioscience, Heidelberg, Germany
Universal PCR Master Mix	Applied Biosystems, Darmstadt, Germany

Table 7. Primers for Real-time PCR

Murine primers	Ordering number	Company
ASC	Mm00445747_g1	Applied Biosystems, Darmstadt, Germany
Caspase1	Mm00438023_m1	Applied Biosystems, Darmstadt, Germany
CCL2	Mm00441242_m1	Applied Biosystems, Darmstadt, Germany
CCL7	Mm004432113_m1	Applied Biosystems, Darmstadt, Germany
Cx3Cr1	Mm02620111-s1	Applied Biosystems, Darmstadt, Germany
Col1a1	Mm01302043_g1	Applied Biosystems, Darmstadt, Germany
Col3a1	Mm00802331_m1	Applied Biosystems, Darmstadt, Germany
GAPDH	Mm99999915_g1	Applied Biosystems, Darmstadt, Germany
LOX	Mm00495386_m1	Applied Biosystems, Darmstadt, Germany
Ly6C	Mm03009946_m1	Applied Biosystems, Darmstadt, Germany
TNF-α	Mm00443258_m1	Applied Biosystems, Darmstadt, Germany

Table 8. Immunohistochemistry staining solutions

Solutions	Composition
1x PBS, 0.075% H_2O_2	500 µL 30%H_2O_2 + 1x PBS ad 200 mL
25x PBS (pH 7.3)	200 g NaCl + 5 g KCl + 6.25 g KH_2PO_4 + 33.75 g Na_2HPO_4*$2H_2O$ + A.dest ad 2000 mL
1x PBS	80 mL 25x PBS + A.dest ad 2000 mL
1x PBS, 10% FBS buffer	1 mL 100% FBS + 9 mL 1xPBS
1.AB solution (dilution of 1:50) for EnVision method	20 µL 1.AB + 980 µL 1x PBS
2.AB solution for EnVision method	2.AB EnVision anti-rabbit is ready-to-use
1x TBS, 0.075% H_2O_2	500 µL 30%H_2O_2 + 1x TBS ad 200 mL
10x BSA	5 g BSA + 1x TBS ad 50 mL
10x TBS (pH 7.6-7.8)	60.6 g Trizma HCl +13.9 g Trizma Base + 87.66 g NaCl + A.dest ad 1000 mL
1x TBS	200 mL 10x TBS + A.dest ad 2000 mL
1x TBS, 0.1% Tween 20	100 mL 10x TBS + 1 mL Tween 20 + A.dest ad 1000 mL
1X TBS, 0.01% Tween 20	100 mL 0.1% Tween 20 + 1x TBS ad 1000 mL
Biotin block for ABC method	100 µL 100% goat serum (GS) + 100µL 10x BSA + 800 µL 1x TBS + 4 drops Avidin solution
1.AB solution (dilution of 1:50) with Avidin block for ABC method	100 µL 10%BSA + 20 µL 1.AB + 880 µL 1x TBS + 4 drops Biotin
2.AB solution (dilution of 1:250) for ABC method	100 µL 10%BSA + 4 µL 2.AB + 896 µL 1x TBS ad 1000 µL
ABC complex for ABC method	1 mL 1x TBS + 1 drop Reagent A + 1 drop Reagent B
0.2 mol Sodium acetate	27.2 Sodium acetate trihydrate + A.dest ad 1000 mL
0.2 mol Acetic acid	11 mL 96-100% Acetic acid + A.dest ad 1000 mL
Carbazole solution	50 mg 3-Amiono-9-ethylcarbazole (AEC) + 10 mL N,N-dimethylformamide + 100 µL 30% H_2O_2 + 35 mL 0.2 mol Sodium acetate solution + 15 mL 0.2 mol Acid acetic solution+ A.dest ad 200 mL

Table 9. Antibodies for immunohistochemistry

Antibody	Company
Anti-ASC	GeneTex, Irvine, CA, USA
Anti-CD4	BD Bioscience, Heidelberg, Germany
Anti-CD8a	BioLegend, Koblenz, Germany
Anti-CD11c	BioLegend, Koblenz, Germany
Anti-CD68	Abcam, Cambridge, Germany
Anti-Collagen I	Chemi-Con, Nuremberg, Germany
Anti-Collagen III	Calbiochem, San Diego, CA, USA

Table 10. Antibodies for flow cytometry

Antibody	Company
Annexin V/7AAD	BioLegend, Koblenz, Germany
Anti-ASC	BioLegend, Koblenz, Germany
Anti-caspase 1 p10	Bioss Antibodies, Woburn, MA, USA
Anti-CAR	Merck KGaA, Darmstadt, Germany
Anti-CCR2	BioLegend, Koblenz, Germany
Anti-CD11b	BioLegend, Koblenz, Germany
Anti-CD68	BioLegend, Koblenz, Germany
Anti-CD115	BioLegend, Koblenz, Germany
Anti-Cx3Cr1	BioLegend, Koblenz, Germany
Anti-IL-1β	BioLegend, Koblenz, Germany
Anti-Ly6C	BioLegend, Koblenz, Germany

3.2. Methods

3.2.1 Study design

3.2.1.1 *In vitro* study

In vitro experiments were performed using the murine cardiomyocyte cell line HL-1. Before cell plating, 6-well plates were first coated with 0.02% Gelatin (Sigma-Aldrich Chemie, Steinheim, Germany) for 30 minutes (min) at 37°C. Afterwards, $2.25x10^5$ cells were plated per well in full Claycomb medium (Sigma-Aldrich Chemie) supplemented with 10% FBS (Biochrom, Berlin, Germany), 1% penicillin/streptomycin (P/S, Life Technologies, Carlsbad, CA, USA), 0.1 mmol/L norepinephrine (Sigma-Aldrich Chemie), and 2 mmol/L L-glutamine (Biochrom). 24 hours (h) later, plates were divided into four groups (control, colchicine, CVB3, and CVB3+colchicine), and infected with CVB3 (Nancy Strain) at a multiplication of infection (m.o.i.) of 2 in serum starvation medium, or incubated with serum starvation medium, both for 1h. One hour post CVB3 infection or serum starvation, cells were incubated in the presence of 100 ng/mL colchicine (Merck Millipore, Darmstadt, Germany) or PBS (Thermo Fisher Scientific). After 4 and 24h of CVB3 infection, cells were collected for subsequent flow cytometry analyses, including the analysis of NLRP3 inflammasome-related proteins (ASC, caspase 1, and IL-1β), CAR, and apoptosis.

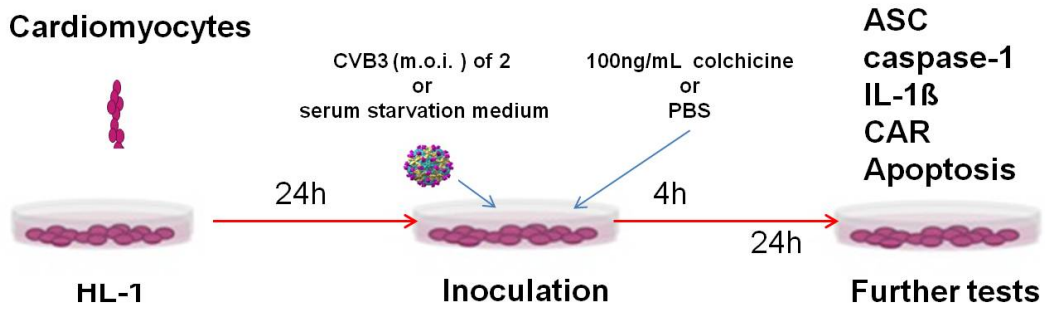

Figure 4. *In vitro* set up for Coxsackievirus B3-infected HL-1 cells stimulated with colchicine.

3.2.1.2 *In vivo* study

Eight-week-old male C57BL6/j mice (Charles Rivers, Sulzfeld, Germany) were randomly divided into four groups (control, colchicine, CVB3, and CVB3+colchicine). The CVB3 and CVB3+colchicine group were infected with $1x10^5$ plaque forming units (p.f.u) of CVB3 (Nancy Strain) in 0.2 mL PBS via intraperitoneal (i.p.) injection. The control and colchicine group were injected with an identical volume of sole PBS. 24h after CVB3 infection, mice were treated either with 5μmol/kg body weight (BW) colchicine (Merck Millipore) or PBS (Thermo Fisher Scientific)

via oral gavage. On day 7, left ventricular (LV) function was assessed via conductance catheter measurements. Subsequently, mice were euthanized, and the left ventricle (LV) and spleen were harvested for further analysis. All experimental procedures were approved by the local authority (Landesamt für Gesundheit und Soziales, Berlin, Germany) and followed the European legislation for the care and use of laboratory animals.

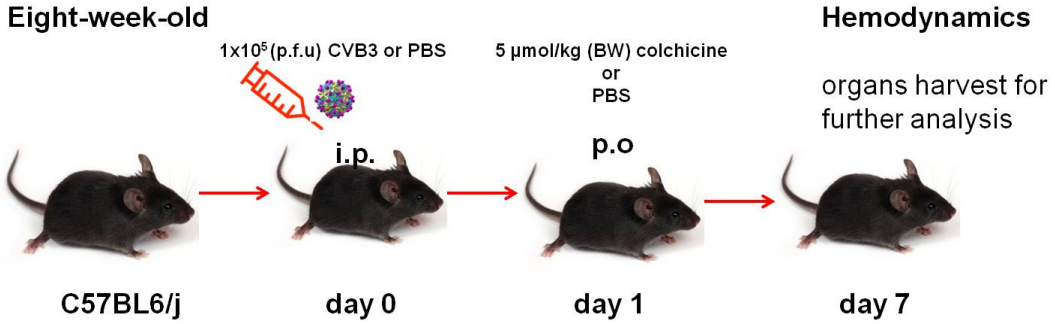

Figure 5. Coxsackievirus B3-induced myocarditis model. Mice were infected with Coxsackievirus B3 (CVB3) via intraperitoneal (i.p.) injection of $1x10^5$ plaque forming units (p.f.u.) of CVB3. Control mice received PBS i.p. One day after infection (day 1), colchicine or PBS were orally (p.o.) administered. Seven days after infection (day 7), mice were first hemodynamically characterized and subsequently euthanized for organ harvest.

3.2.2. Characterization of cardiac function by conductance catheter

3.2.2.1. Theoretical background of the conductance catheter technique

Simultaneous determination of LV pressure (P) and LV volume (V) is a comprehensive method to obtain quantitative hemodynamic parameters in real-time. A variety of relevant cardiac parameters such as stroke volume (SV), ejection fraction (EF), and LV contractility (dP/dt_{max}) are derived from PV loops.

The principle of this measurement is the relationship between the time-varying LV conductance and the time-varying change in LV V. The conductance is the reciprocal of the electrical resistance, which depends on the V of the LV. By generating an electric field, changes of the electric potential, indirectly reflecting V changes, can be measured. However, measured conductance consists of the parallel conductance from the LV wall and blood. Injection of 10% saline solution (Fresenius Kabi AG, Bad Homburg, Germany) via the jugular vein enables the determination of the parallel conductance from the blood to obtain the real LV volume [85].

3.2.2.2 Anesthesia

First, mice were anesthetized by a mixture of 0.8-1.2 g/kg urethane (Indivior UK Limited, Slough, UK) and 0.05 mg/kg buprenorphine (Sigma-Aldrich) via i.p. injection. The depth of the anesthesia was monitored by checking the response to tail and paw pinch.

3.2.2.3. Intubation and ventilation

Afterwards, mice were fixed in the supine position with their necks in hyperextension on a surgical platform. To expose the trachea, a cervical incision was made and the surrounding tissue was removed. Next, a 22G cannula was inserted into the trachea and immediately connected to a ventilator. Stroke volume was determined by body weight (BW, 6.5 mL/kg BW) and the ventilation rate was set about 200 (breaths/min).

3.2.2.4. Open-chest method

After starting the artificial ventilation, the chest was opened in diaphragmatic direction to avoid injuring inner organs such as intestine, liver, and lungs. To expose the LV, the diaphragm was opened and the pericardium from the heart gently removed. By puncturing the apex with a 26G needle, the conductance catheter was inserted into the LV [86].

3.2.2.5. Recording of pressure-volume loops

Once the catheter was inserted into the LV at an appropriate position, PV loops were recorded. The system consists of a 1.2 French conductance catheter (Scisense, Ontario, Canada), a MPVS 300/400 amplifier (Millar Instruments, Houston, TE, USA), and the IOX 1.8.9 operation software (EMKA, Technologies, Falls Church, VI, USA). For data analysis, the program Circlab 2004 (Millar Instruments) was used.

For this study, the basic LV pump function (steady state) was first recorded. To calculate the parallel conductance of the LV, 5-10 μL of hypertonic saline solution (10%) was injected. Additionally, the vena cava was occluded to determine load-independent parameters. During the recording, the ventilator was shut off to avoid lung motion artifacts affecting the measurement. All measurements were repeated three times with a short interval between the recordings.

3.2.2.6. Main parameters for cardiac hemodynamic function

Table 11. Parameters for cardiac hemodynamics

Parameter	Description	Unit
EF	ejection fraction; EF = SV/ LVEDV × 100%	%
CO	Cardiac output; the blood volume ejected from the LV per min; CO = HR × SV	μl /min
LVP_{max}	maximum LV pressure during systole.	mmHg
dP/dt_{max}	LV contractility; the maximal rate of rise in LV pressure (LVP) during isovolumetric contraction	mmHg/s
dP/dt_{min}	LV relaxation; the minimum LVP decay rate during isovolumetric relaxation	mmHg/s
Tau	LV relaxation time; exponential decay of the LVP during isovolumetric relaxation	ms

3.2.3. Molecular methods for real-time polymerase chain reaction

3.2.3.1. RNA extraction

To isolate total RNA from tissue samples, the TRIzol method was performed. RNA extraction includes homogenization of the samples, phase separation, precipitation, washing and purification. First, frozen samples were placed in a FACS tube containing 1 mL TRIzol reagent, and subsequently homogenized. Afterwards, the homogenized samples were transferred into a 1.5 mL tube and 200 µL Chloroform was added. Samples were vigorously shaken for 15 seconds (sec), incubated at room temperature (RT) for 2 min, followed by centrifugation at 10,000 rpm for 15 min at 4°C. After the centrifugation, the mixture was separated into three phases: a red chloroform phase on the bottom, a white interphase, and a colorless upper phase, containing the RNA. Next, the upper phase was carefully transferred into a new 1.5 mL tube. Then, 500 µL of isopropanol (100%) was added. The tubes were gently shaken and incubated at RT for 15 min, followed by centrifugation at 10,000 rpm for 10 min at 4°C to precipitate the RNA. Subsequently, the RNA pellet was washed with 500 µL ethanol (70%). Afterwards, samples were mixed, followed by centrifugation at 7,500 rpm for 10 min at 4°C. The supernatant was discarded and the RNA pellets were air dried for 5-10 min. By adding 100 µL RNase-free water, the pellet was re-solved. Finally, the NucleoSpin® RNA mini kit (Macherey-Nagel GmbH, Düren, Germany) was used for RNA purification. In brief, each 100 µL RNA sample was supplemented with lysis-binding buffer (300 µL RA1 + 300 µL 96% ethanol). Then, the lysate was loaded on a NucleoSpin® RNA II column and centrifuged at 12,000 rpm for 30 sec. After centrifugation, columns were placed in a collection tube with 350 µL membrane desalting buffer, followed by another centrifugation at 12,000 rpm for 1 min. For DNAse treatment, 95 µL DNase reaction mixture was added on the column and incubated for 15 min at RT. Subsequently, the silica membranes were washed three times and centrifuged according the manufactures protocol. To elute the RNA, 50 µL of RNase-free water was added to the columns and the tubes were centrifuged at 12,000 rpm for 1 min. Finally, the RNA yield was measured by determination of the absorbance at 260 nm using a NanoDrop 1000. Isolated RNA was stored at -80°C or directly used for reverse transcription.

3.2.3.2. Reverse Transcription

The High Capacity cDNA Reverse Transcription Kit (Applied Biosystems, Darmstadt, Germany) was used to perform reverse transcription, synthesizing complementary DNA (cDNA) from mRNA. All procedures followed the manufacturer's protocol. Briefly, RNase-free water was added to 1 µg RNA, reaching a total volume of 11 µL. Next, solution was mixed with 2.8 µL random primers and dNTPs, followed by heating for 5 min at 70°C in a thermocycler. Meanwhile, a master-mix solution composed of 2 µL Buffer, 3.2 µL RNase-free water, and 1 µL reverse transcriptase was prepared. The heated tubes were directly transferred on ice and mixed with 6.2 µL of the master-mix solution, followed by a second incubation in the thermocycler. The heating program was the following: 1) incubation for 10 min at 25°C, 2) 2 h heating at 37°C, 3) 5 min heating at >85°C, and 4) cool down at 4°C to terminate the reaction. Finally, 30 µL RNase-free water was added to dilute cDNA to a final volume of 50 µL for subsequent real-time polymerase chain reaction (PCR).

3.2.3.3. Real-time polymerase chain reaction

Real-time PCR was performed to evaluate gene expression of LV tissue samples. Amplification and data analysis was performed on the Quant studio 6 Flex TaqMan real-time PCR system (Life Technologies, Darmstadt, Germany). Therefore, 10 µL final reaction mixture composed of 5 µL PCR master mix, 0.5 µL gene reporter assay, 3.5 µL water and 1 µL cDNA was used. The amplification program was the following: first, heating at 50°C for 2 min, followed by denaturation at 95°C for 10 min. Then, second denaturation at 95°C for 15 sec, followed by annealing and elongation at 60°C for 1 min. Depending on the target gene, 40 or 45 cycles were carried out. In this study, expression of fibrosis-related genes (LOX, Col1a1, and Col3a1), chemokine-related genes (CCL2, CCL7, and Cx3Cr1), immune response-related genes (Ly6C, NLRP3, ASC, caspase 1, and TNF-α), and CVB3 was analyzed and normalized towards the housekeeping gene GAPDH.

3.2.4. Immunohistochemistry

3.2.4.1. Generation of frozen tissue sections

Before cutting, LV tissue samples were transferred from -80°C to -20°C overnight. LV samples were embedded in Tissue-Tek OCT media and cut on a Cryostat into 5 µm thick sections. Subsequently, the sections were immersed in ice-cold acetone for 10 min. After drying, the slides were immediately used for staining or stored at -20°C.

3.2.4.2. Immunohistochemistry staining

The core principle of immunohistochemistry (IHC) is a visible antigen-antibody specific binding, which can be quantitatively analyzed under a microscope. In this study, two methods were used: the EnVision® method and the Avidin-biotin complex (ABC) method, depending on the investigated antigen (**Table 12**).

Table 12. Antibodies for immunohistochemistry

1. AB	Species	Dilution	2. AB	Species	Dilution	Method
ASC	Rabbit	1:100	EnVision	Anti-Rabbit	undiluted	EnVision
CD4	Rat	1:50	Dianova	Anti-Rat	1:250	ABC
CD8	Rat	1:50	Dianova	Anti-Rat	1:250	ABC
CD11c	Rat	1:50	Dianova	Anti-Rat	1:250	ABC
CD68	Rabbit	1:600	Dianova	Anti-Rabbit	1:250	ABC
Col1	Rabbit	1:350	EnVision	Anti-Rabbit	undiluted	EnVision
Col3	Rabbit	1:200	EnVision	Anti-Rabbit	undiluted	EnVision

1. AB=primary antibody, 2. AB=secondary antibody, Col1=Collagen I, Col3= Collagen III.

3.2.4.2.1. EnVision method

The EnVision method comprises a two-step staining. First, specific binding of the primary antibody (1.AB) with the antigen, followed by coupling with the secondary antibody (2.AB) labeled with a species-specific horseradish peroxidase (HRP). Second, a substrate-chromogen for HRP makes the antigen-antibody complex visible. Thus, this method has the advantage of

avoiding nonspecific staining resulting from endogenous avidin-biotin activity compared to the avidin-biotin complex (ABC) method.

The detailed protocol is as follows: the slides were immersed in 1xPBS on a shaker for 5 min to adapt slices to the buffer milieu. Afterwards, slides were transferred to freshly prepared 0.075% H_2O_2 solution for 7 min on a shaker to block endogenous peroxidase. Next, slides were again washed with 1xPBS. Afterwards, 75 µL of the 1.AB solution was added for each staining area and incubated for 1 h in a humidity chamber. Subsequently, slides were washed twice with 1xPBS before the 2.AB solution was added. After 30 min incubation, slides were washed twice, followed by incubation with fresh carbazole solution for 12 min in the dark to visualize the peroxidase of the 2.AB. Then, slides were again washed twice with 1xPBS and subsequently stained with Hemalum for 30 sec. After the incubation, slides were first rinsed several times under tap water and second, they were moved into hot tap water (50-60°C) for 10 min. Finally, Kaiser´s glycerol gelatin was used to mount the slides for further storage and analysis.

3.2.4.2.2. Avidin-biotin complex method

In this study, the avidin-biotin complex (ABC) method was used to determine the presence of inflammatory cells in the LV. The most important advantage of the ABC method is an improved sensitivity to the target antigen due to an extraordinary affinity of avidin to biotin. The multiple biotin-binding sites in each tetravalent avidin molecule are ideal for achieving this amplification via forming a complex (**Figure 6**).

The detailed protocol is the following: the complete ABC method was performed using 1x TBS buffer milieu. First, slides were immersed in 1xTBS for 5 min, followed by blocking with 0.075% H_2O_2 for 7 min. Afterwards, slides were washed with 1xTBS for 5 min on the shaker. Meanwhile, the avidin-goat serum solution was prepared and 75 µL for each staining field was added after the washing step. By this step, the endogenous biotin was blocked and electrostatic interaction and unspecific binding were avoided, respectively. After 30 min incubation, the 1.AB solution was added for an additional 60 min. To avoid unspecific binding and to block the endogenous avidin, 1% bovine serum albumin (BSA) and biotin were added to the solution. Afterwards, slides were washed twice with 1xTBS for 5 min on a shaker. In the next step, biotinylated 2.AB was incubated for 60 min, followed by two-time washing with 1xTBS supplemented with 0.01%

Tween 20 (Sigma-Aldrich) to reduce the hydrophobic surface of the slides. Each washing step was performed for 5 min on the shaker. To form the ABC complex by binding of HRP-labeled avidin to the biotinylated 2.AB, the respective solution was prepared 30 min in advance and added after washing. 75 µL of the ABC solution was added per staining field and incubated for 30 min. Then, slides were washed twice with 1xTBS on the shaker. Similar to the EnVision method, slides were stained with Hemalum, washed and finally mounted with Kaiser´s glycerol gelatin.

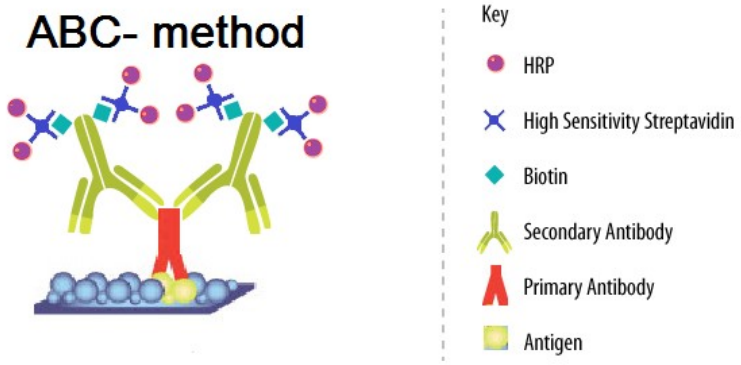

Figure 6. Illustration of the avidin-biotin complex [87]. The avidin-biotin complex (ABC) method is the most common method for amplifying a target antigen. This method uses streptavidin and biotinylated secondary antibody (2.AB), which binds to the primary antibody (1.AB).

3.2.5. Flow cytometry

Via flow cytometry, single cells can be measured and analyzed via the expression of cell surface or intracellular markers. Within this study, cells were determined by the expression of Annexin $V^+/7AAD^-$, ASC, CAR, Caspase 1, CCR2, CD11b, CD68, CD115, Cx3Cr1, IL-1β, and Ly6C. All samples were measured on a MACSQuant Analyzer (Miltenyi Biotec， Bergish Gladbach, Germany) and analyzed via the FlowJo software version 8.8.6. (Tree Star Inc., Ashland, VI, USA). Data are expressed as percentage (%) of gated cells.

Table 13. Antibodies for flow cytometry

Antibody	Labelling
Annexin V/7AAD	FITC
Anti-ASC	PE
Anti-caspase 1 p10	Alexa Fluor 488
Anti-CAR	PE
Anti-CCR2	Alexa 647
Anti-CD11b	Brilliant Violet 421
Anti-CD68	PerCP/Cy5.5
Anti-CD115	Alexa Fluor
Anti-Cx3Cr1	PE
Anti-IL-1β	APC
Anti-Ly6C	Brilliant Violet 421

3.2.5.1. Annexin $V^+/7AAD^-$ staining for the measurement of apoptotic HL-1 cells

According to the *in vitro* set up (**3.2.1.1**), HL-1 cells were infected and stimulated with colchicine. At the stipulated time points, cells were harvested and washed twice with cold cell staining buffer (Biolegend, Koblenz, Germany). After the last washing step, cells were re-suspended in 100 µL Annexin-binding buffer (BioLegend). Next, 5 µL anti-Annexin V and 5 µL of anti-7AAD were added and incubated at RT for 15 min in the dark. After incubation, 400 µL Annexin-binding buffer was added for measurement.

3.2.5.2. ASC, IL-1β, CAR and caspase 1 expression of HL-1 cells

At the stipulated time points, $1x10^6$ HL-1 cells were fixed and permeabilized in 500 µL Cytofix/Cytoperm buffer (BD Biosciences, Heidelberg, Germany) for 20 min at 4°C. Afterwards, cells were washed with 500 µL Perm/Wash buffer (BD Biosciences), followed by centrifugation at 3,000 rpm for 5 min. Cells were re-suspended in 96 µL Perm/Wash buffer (BD Biosciences) and 2 µL anti-IL-1β and 2 µL anti-ASC antibodies were added for incubation at RT for 30 min in the dark. For caspase 1 (p10), cells were re-suspended in 97 µL Perm/Wash buffer (BD Biosciences). Subsequently, 3 µL of anti-caspase 1 (p10) antibody was added, followed by 30-60 min incubation at 37°C. Next, cells were washed with PBS und re-suspended in 200µl PBS for flow cytometry analysis. For the analysis of CAR, cells were re-suspended in 98 µl PBS, and 2µl anti-CAR antibody was added and incubated for 20 min at 4°C. After washing and centrifugation, samples were re-suspended in 200 µL PBS and analyzed.

3.2.5.3. Preparation of splenocytes

The collected spleens were first positioned in a Petridish with RPMI medium (Gibco/Thermo Fisher Scientific) and afterwards transferred on a 70 µm cell strainer placed on a 50 mL Falcon tube. With the plunger of a 2.5 mL syringe, the spleen was smashed through the cell strainer, followed by flushing the strainer with up to 15 mL PBS (Thermo Fisher Scientific) supplemented with 1% FBS. The suspension was homogenized and centrifuged at 3,500 rpm for 5 min at RT. After centrifugation, the cell pellet was re-suspended in 6 mL ACK lysis buffer (Gibco/ Thermo Fisher Scientific) and incubated for 4 min at RT. By adding 40 mL RPMI medium, the lysis of erythrocytes was stopped. The suspension was now passed through a 40 µm cell strainer and again centrifuged at 3,500 rpm for 5 min. Finally, the pellet was either re-suspended in PBS for subsequent staining, or in FBS supplemented with 10% DMSO (Merk Millipore) for freezing.

3.2.5.4. Investigation of splenic monocyte subsets

To analyze the different splenic monocyte subsets [88], $1x10^6$ cells were re-suspended in 85.5 µL MACS staining Buffer (Miltenyi Biotec), containing 5µL anti-Ly6C, 2 µL anti-CD115, 2.5 µL anti-CD11b, 2.5 µl anti-Cx3Cr1 and 2.5 µl anti-CCR2 or 2.5µL CD68 antibodies. Antibodies were

incubated at 4°C for 20 min in the dark, followed by washing and centrifugation. Finally, samples were re-suspended in 100 µL PBS for subsequent measurement.

3.2.5.5. Isolation of cardiac mononuclear cells

Cardiac mononuclear cells were isolated from control, colchicine, CVB3 and CVB3+ colchicine mice using the Neonatal Heart Dissociation Kit (Miltenyi Biotec, Bergisch Gladbach, Germany) and gentleMACS Octo Dissociator (Miltenyi Biotec, Bergisch Gladbach, Germany), according to the manufacturer's instructions.

3.2.5.6. Evaluation of ASC-, caspase 1-, and IL-1β-expressing cardiac mononuclear cells

Isolated cardiac mononuclear cells (MNCs) were re-suspended in 1x Cytofix/Cytoperm buffer (BD Biosciences, Heidelberg, Germany) and stained with 2 µL anti-ASC, 2 µL anti-caspase 1 p10 and 2 µL anti-IL-1β, and incubated for 30 min at RT. Next, cells were washed with 500 µL PBS and analyzed via flow cytometry.

3.2.6. Statistical analysis

Statistical analysis was performed using GraphPad Prism 7.0 software (GraphPad Software, La Jolla, CA, USA). Data are expressed as mean±SEM and were compared with the One-way ANOVA and Sidak´s *post hoc* test. Differences were considered statistically significant at a value of $p<0.05$.

4. Results

4.1. *In vitro* study

4.1.1 Impact of colchicine on apoptosis of Coxsackievirus B3-infected HL-1 cells

CVB3 infection induces HL-1 cardiomyocyte apoptosis, leading to viral progeny release [89]. To assess the impact of CVB3 infection on HL-1 apoptosis, cells were stained with the Annexin V and 7AAD staining kit and subsequently analyzed via flow cytometry. Early stage apoptotic cells were identified as Annexin V^+ and $7AAD^-$. CVB3 infection increased the percentage of early apoptotic cells by 2.8-fold ($p<0.0001$) compared to control cells (**Figure 7**). Furthermore, colchicine partly abrogated this CVB3-induced detriment on HL-1 cells as indicated by 1.4-fold ($p<0.0001$) lower Annexin V^+ / $7AAD^-$ cells in colchicine-treated CVB3-infected cells than in untreated CVB3-infected cells (**Figure 7**).

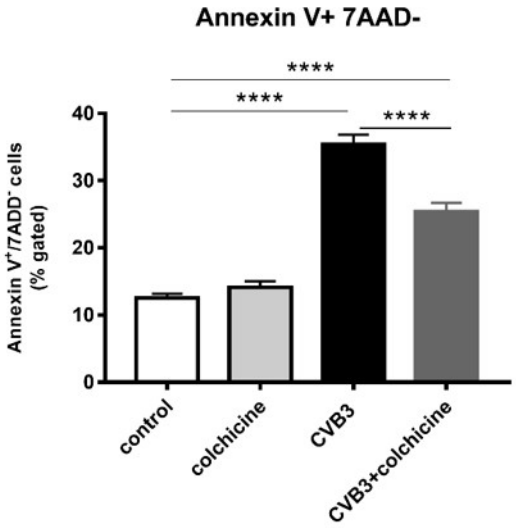

Figure 7. Colchicine reduces apoptosis of Coxsackievirus B3-infected HL-1 cells. Bar graph represents mean±SEM of the % of apoptotic cells indicated as Annexin $V^+/7AAD^-$ of control, colchicine, Coxsackievirus B3-infected (CVB3) and CVB3-infected HL-1 cells treated with colchicine (CVB3+colchicine), 24 hours post CVB3 infection. Statistical analysis was performed by One-way ANOVA (****$p<0.0001$, with n=6/group for control, colchicine, CVB3, and CVB3+colchicine).

4.1.2. Impact of colchicine on Coxsackievirus and Adenovirus Receptor expression of Coxsackievirus B3-infected HL-1 cells

CAR is a key receptor enabling CVB3 to enter into the cardiomyocyte [90]. In this study, CAR expression was measured via flow cytometry. As shown in Figure 8, CAR surface expression

on HL-1 cells was 1.9-fold ($p<0.0001$) and 5.9-fold ($p<0.0001$) increased 4h and 24h after CVB3 infection versus uninfected controls, respectively (**Figure 8, A-B**). Compared to untreated CVB3-infected cells, colchicine reduced CAR expression by 1.7-fold ($p<0.001$) and 1.4-fold ($p<0.001$) after 4h and 24h, respectively (**Figure 8, A-B**).

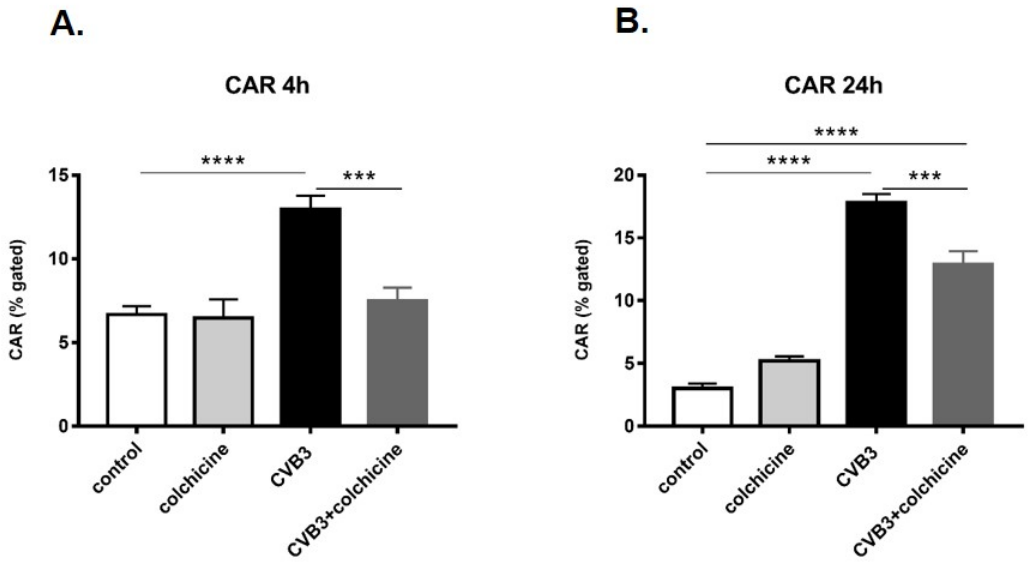

Figure 8. **Colchicine reduces Coxsackievirus and Adenovirus receptor expression on Coxsackievirus B3-infected HL-1 cells.** Bar graphs represent the mean±SEM of the Coxsackievirus and Adenovirus receptor (CAR) expression of control, colchicine, Coxsackievirus B3-infected (CVB3) and CVB3-infected HL-1 cells treated with colchicine (CVB3+colchicine), **A.** 4 hours (h) and **B.** 24h post CVB3 infection HL-1 cells. Statistical analysis was performed by One-way ANOVA (***$p<0.001$, ****$p<0.0001$, with n=6/group for control, colchicine, CVB3, and CVB3+colchicine).

4.1.3. Impact of colchicine on the NLRP3 inflammasome of Coxsackievirus B3- infected HL-1 cells

In HL-1 cells, the NLRP3 inflammasome-associated proteins ASC, caspase 1, and IL-1β were investigated via flow cytometry. ASC, caspase 1, and IL-1β were 1.8-fold ($p<0.0001$), 1.4-fold ($p<0.0001$), and 3.2-fold ($p<0.0001$) increased in CVB3-infected cells compared to uninfected controls, respectively (**Figure 9**). In addition, ASC, caspase 1, and IL-1β were 1.3-fold ($p<0.01$), 1.2-fold ($p=0.001$), and 2.0-fold ($p<0.0001$) reduced in colchicine-treated CVB3-infected cells versus untreated CVB3-infected cells, respectively (**Figure 9**).

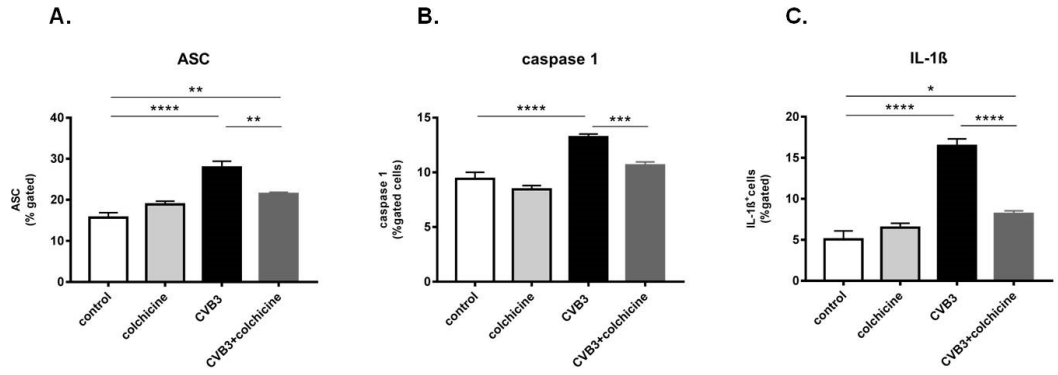

Figure 9. Colchicine decreases the expression of components of the NLRP3 inflammasome in Coxsackievirus B3-infected HL-1 cells. Bar graphs represent the mean±SEM of the percentage of **A.** ASC-, **B.** caspase 1-, and **C.** IL-1β-positive cells of control, colchicine, Coxsackievirus B3-infected (CVB3) and CVB3-infected HL-1 cells treated with colchicine (CVB3+colchicine), 4 hours post CVB3 infection. Statistical analysis was performed by One-way ANOVA (*p<0.05, **p<0.01, ***p≤0.001, ****p<0.0001, with n=6/group for control, colchicine, CVB3, and CVB3+colchicine).

4.2. *In vivo* study

4.2.1. Impact of colchicine on body weight in Coxsackievirus B3-induced myocarditis mice

BW is a simple but useful parameter to predict the health of mice. In this study, CVB3-induced myocarditis led to noticeable mouse weight loss. On day 7, the BW was 1.3-fold ($p<0.01$) lower in CVB3-infected than in uninfected control mice. No significant differences in BW were observed between colchicine-treated CVB3-infected mice and untreated CVB3-infected mice (**Figure 10**).

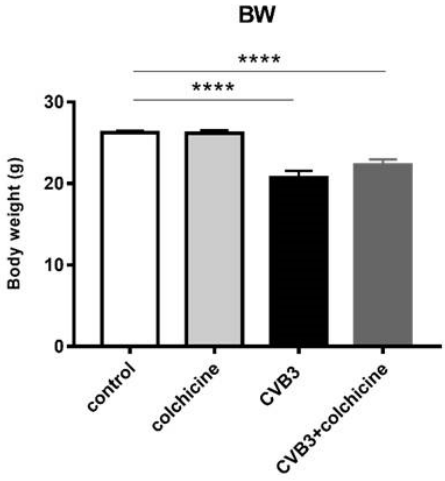

Figure 10. Colchicine does not affect the body weight in Coxsackievirus B3-induced myocarditis mice. Bar graphs represent the mean±SEM of body weight (BW) of control, colchicine, Coxsackievirus B3-infected (CVB3) and CVB3-infected mice treated with colchicine (CVB3+colchicine). Statistical analysis was performed by One-way ANOVA. (****p<0.0001, with n=12 for control group, n=15 for colchicine and CVB3 groups, n=18 for CVB3+colchicine group).

4.2.2. Impact of colchicine on left ventricular function in Coxsackievirus B3-induced myocarditis in mice

CVB3-induced myocarditis impaired both the contraction and relaxation of the LV as shown by a 1.2-fold ($p<0.01$), 2.1-fold ($p<0.01$), 1.4-fold ($p<0.0001$), 2.1-fold ($p<0.0001$), and 2.4-fold ($p<0.0001$) decline in EF, CO, LVP_{max}, dP/dt_{max}, and dP/dt_{min} compared to uninfected control mice, respectively (**Figure 11, A-E**). Colchicine partly abrogated the adverse effects on LV function in CVB3-infected mice. EF, CO, LVP_{max}, dP/dt_{max}, and dP/dt_{min} were 1.1-fold ($p<0.05$), 1.8-fold ($p<0.05$), 1.5-fold ($p<0.001$), 2.0-fold ($p<0.001$), and 2.1-fold ($p<0.0001$) higher in CVB3+colchicine mice than in untreated CVB3-infected mice, respectively (**Figure 11, A-E**). Meanwhile, Tau was 2.3-fold ($p<0.0001$) higher in the CVB3-infected versus uninfected mice. Colchicine lowered Tau by 1.9-fold ($p<0.0001$) in CVB3-infected mice (**Figure 11F**). There were no significant differences in hemodynamic LV function observed between sole colchicine-treated mice and control mice (**Figure 11, A-F**).

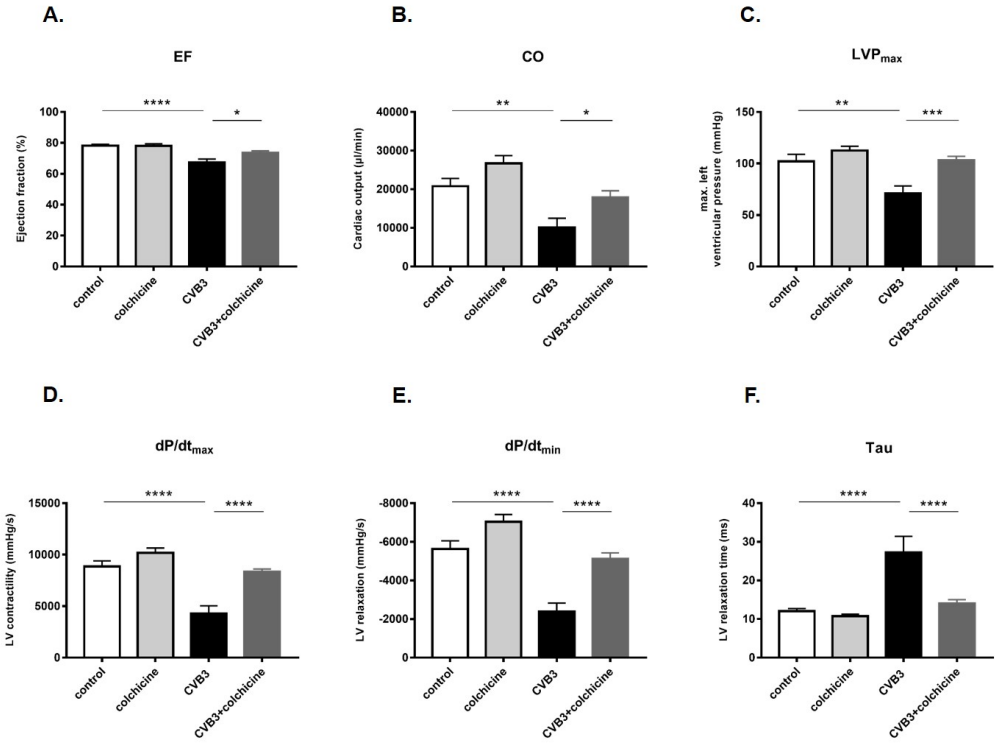

Figure 11. Colchicine improved left ventricular function in Coxsackievirus B3-induced myocarditis mice. Bar graphs represent the mean±SEM of **A.** EF (%), **B.** CO (µl/min), **C.** LVP_{max} (mmHg), **D.** dP/dt_{max} (mmHg/s), **E.** dP/dt_{min} (mmHg/s), and **F.** Tau (ms) of control, colchicine, Coxsackievirus B3-infected (CVB3) and CVB3-infected mice treated with colchicine (CVB3+colchicine). Statistical analysis was performed by One-way ANOVA. (*$p<0.05$, **$p<0.01$, ***$p<0.001$, ****$p<0.0001$, with n=11 for control group, n=13 for colchicine and CVB3 groups, n=16 for CVB3+colchicine).

4.2.3. Impact of colchicine on cardiac fibrosis in Coxsackievirus B3-induced myocarditis mice

CVB3-induced myocarditis increased cardiac fibrosis as indicated by the 3.9-fold ($p<0.0001$), 3.1-fold ($p<0.05$), and 33-fold ($p<0.0001$) higher LV Col 1a1, Col3a1, and LOX mRNA expression in CVB3-infected compared to uninfected control mice, respectively (**Figure 12, A-C**). Colchicine intervention inhibited the expression of cardiac fibrosis-associated genes. This follows from the 1.9-fold ($p<0.01$) and 4.6-fold ($p<0.001$) lower LV Col1a1 and LOX mRNA expression in CVB3+colchicine mice versus untreated CVB3-infected mice, respectively (**Figure 12, A,C**). Additionally, Collagen I- and Collagen III-positive areas in the LV were assessed via IHC staining and subsequent digital image analysis. CVB3-induced myocarditis did not increase LV collagen I and collagen III deposition. However, a 2.1-fold ($p<0.01$) higher collagen I/III ratio was observed in CVB3-infected compared to uninfected control mice (**Figure 12F**). Colchicine increased LV Collagen III as shown by 1.4-fold ($p<0.05$) higher collagen III in colchicine-treated CVB3-infected mice compared to untreated CVB3-infected mice, but did not affect either collagen I, or the collagen I/III ratio (**Figure 12, D-F**). There was no notable difference in cardiac fibrosis between the colchicine and control mice.

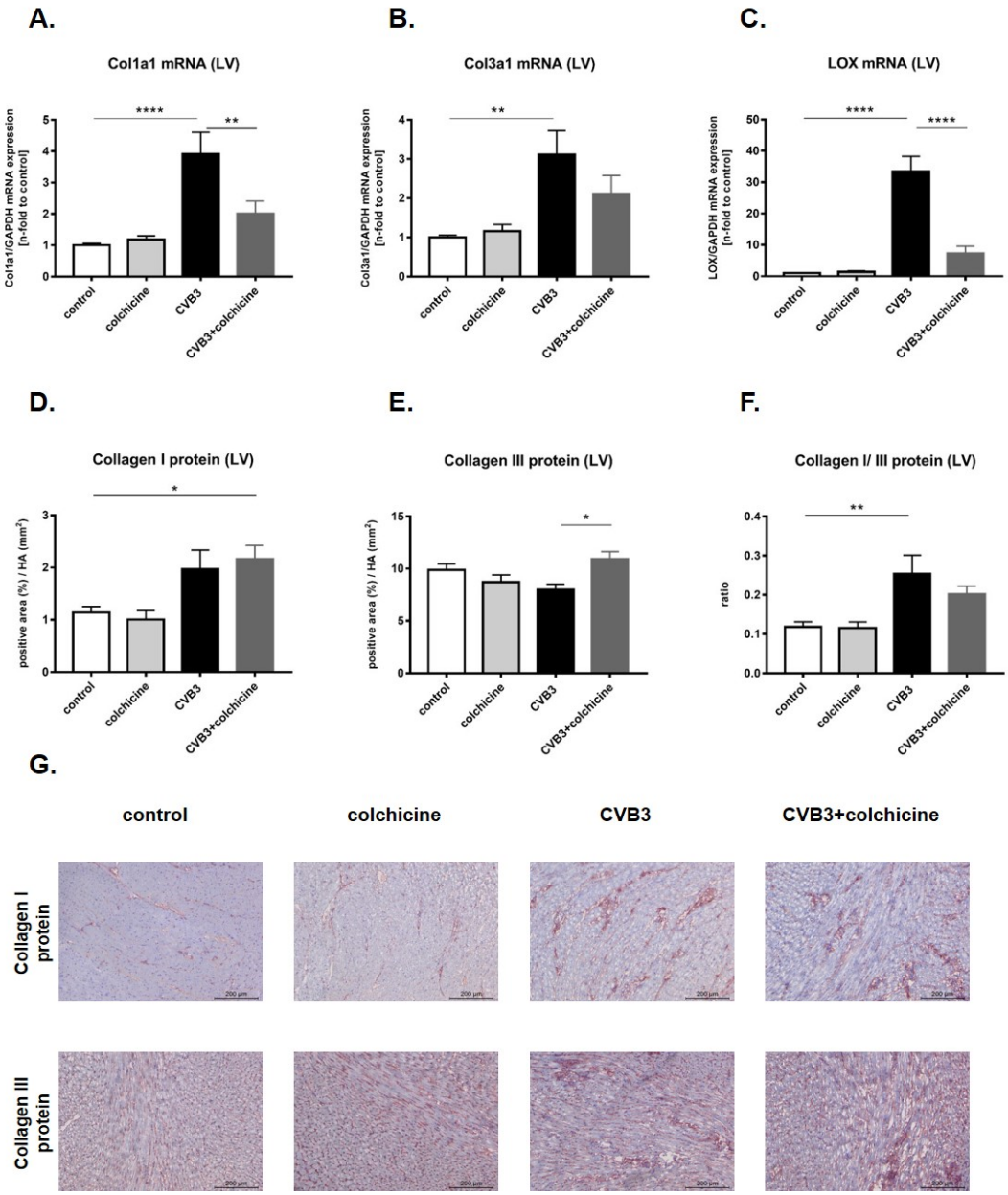

Figure 12. Colchicine decreases cardiac fibrosis in Coxsackievirus-induced myocarditis mice. A.-C. Bar graphs represent the mean±SEM of LV Col1a1, Col3a1 and LOX mRNA expression in control, colchicine, Coxsackievirus B3-infected (CVB3) and CVB3-infected mice treated with colchicine (CVB3+colchicine). **D.-F.** Bar graphs represent the mean±SEM of collagen I, collagen III and collagen I/III ratio of LV collagen deposition in control, colchicine, CVB3 and CVB3+colchicine mice. Statistical analysis was performed by One-way ANOVA. (*p<0.05, **p<0.01, ***p<0.001, ****p<0.0001, with n=12 for control group, n=15 for colchicine and CVB3 groups, n=14 for CVB3+colchicine group). **G.** Representative images of Collagen I- and III-stained LV sections at 100× magnification of control, colchicine, CVB3 and CVB3+colchicine mice.

4.2.4. Impact of colchicine on left ventricular chemokine and chemokine-receptor expression in Coxsackievirus B3-induced myocarditis mice.

In this study, LV mRNA expression of chemokine (C-C motif) ligand 2 (CCL2), chemokine (C-C motif) ligand 7 (CCL7), and CX3C chemokine receptor 1 (Cx3cr1) was measured. These chemokines/chemokine receptors play an important role in the recruitment and migration of monocytes and are of relevance in myocarditis [91, 92]. LV CCL7 mRNA expression was 41-fold ($p<0.05$) increased in CVB3-infected versus uninfected control mice (**Figure 13B**). LV mRNA expression of CCL2, CCL7, and Cx3Cr1 was significantly increased in colchicine-treated CVB3-infected mice compared to uninfected control mice (**Figure 13, A-C**). There was no difference in LV CCL2 and CCL7 mRNA expression between colchicine-treated CVB3-infected and untreated CVB3-infected mice (**Figure 13, A-B**). Interestingly, colchicine promoted LV Cx3Cr1 mRNA expression in CVB3-infected mice, as indicated by 1.8-fold ($p<0.05$) higher LV Cx3Cr1 mRNA expression in CVB3+colchicine compared to CVB3 mice (**Figure 13C**).

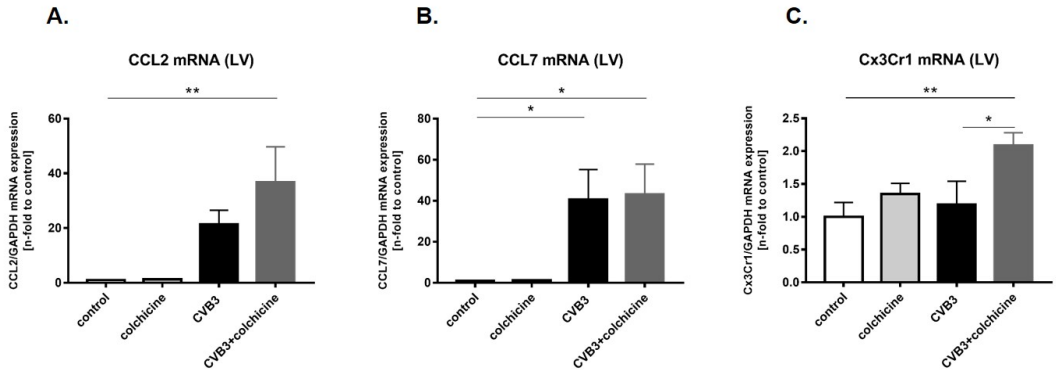

Figure 13. Colchicine affects the left ventricle CCL2, CCL7, and Cx3cr1 mRNA expression in Coxsackievirus B3-infected mice. Bar graphs represent the mean±SEM of LV CCL2, CCL7 and Cx3Cr1 mRNA expression in control, colchicine, Coxsackievirus B3-infected (CVB3) and CVB3-infected mice treated with colchicine (CVB3+colchicine). Statistical analysis was performed by One-way ANOVA. (*$p<0.05$, **$p<0.01$, with n=12 for control and CVB3 groups, n=15 for colchicine group, n=14 for CVB3+colchicine group).

4.2.5. Impact of colchicine on Coxsackievirus B3-induced cardiac inflammation

4.2.5.1. Impact of colchicine on CD4, CD8, and CD11c immune cell presence in the left ventricle

The extent of LV inflammation was assessed by evaluating the presence of immune cells including CD4 and CD8 lymphocytes and CD11c dendritic cells in the LV via IHC. CD4 and

CD11c cells were 3.9-fold ($p<0.05$) and 17-fold ($p<0.01$) higher in the LV of CVB3-infected mice compared to uninfected control mice, respectively (**Figure 14, A,C**). Colchicine did not reduce CD4, CD8 and CD11c cell presence in the LV of CVB3-infected mice (**Figure 14, A-C**).

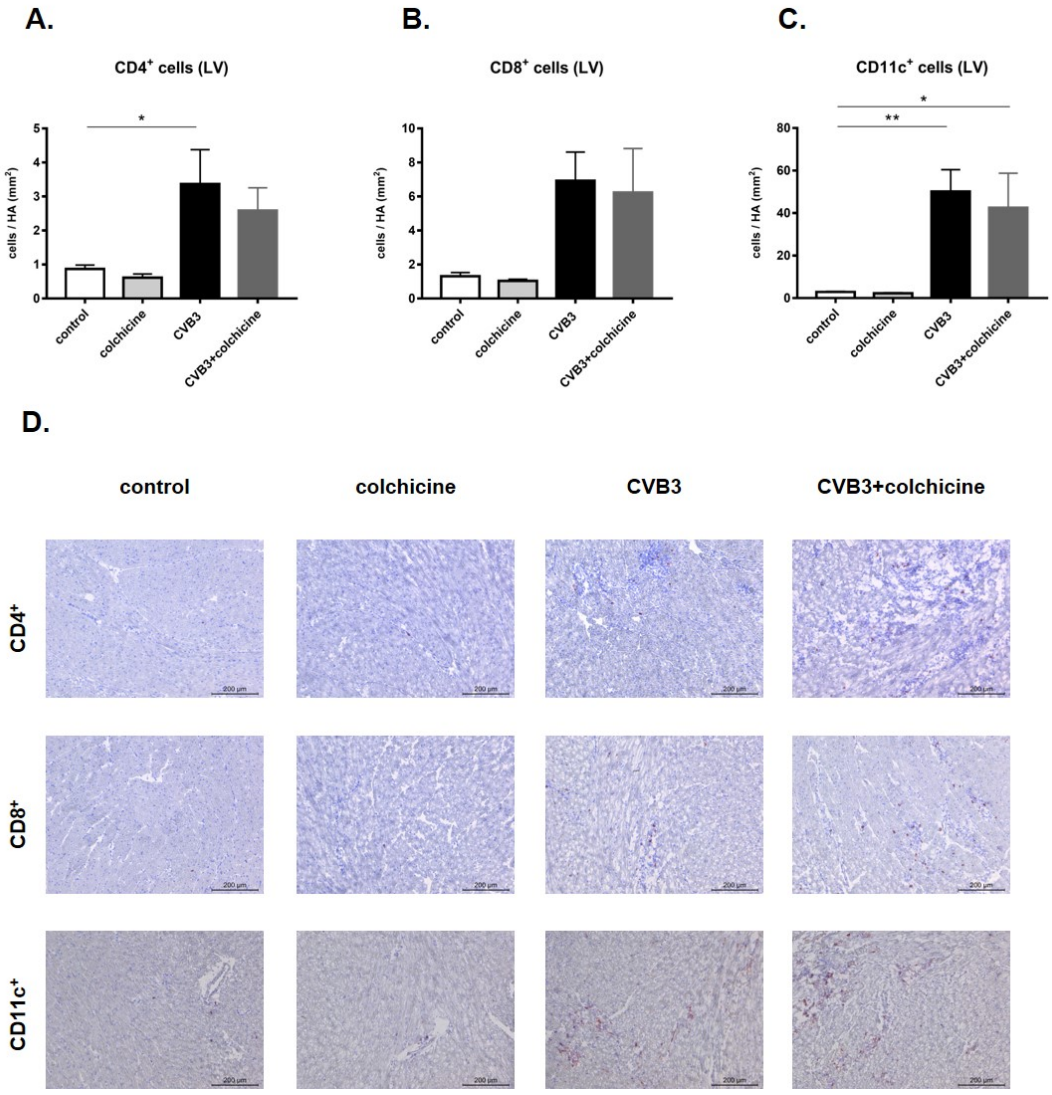

Figure 14. Impact of colchicine on the presence of CD4, CD8, and CD11 immune cells in the left ventricle of Coxsackievirus B3-induced myocarditis mice. A-C. Bar graphs represent the mean±SEM of CD4, CD8, and CD11 immune cell presence depicted as cells/mm^2 in the LV of control, colchicine, Coxsackievirus B3-infected (CVB3) and CVB3-infected mice treated with colchicine (CVB3+colchicine). Statistical analysis was performed by One-way ANOVA. (*$p<0.05$, $p<0.01$, with n=12 for control, n=15 for colchicine and CVB3 groups, n=18 for CVB3+colchicine group). **D.** Representative images of CD4-, CD8-, and CD11c-stained LV sections, at 100× magnification of control, colchicine, CVB3 and CVB3+colchicine mice.

4.2.5.2. Impact of colchicine on CD68 monocytes/macrophages in the spleen and left ventricle of Coxsackievirus B3-induced myocarditis mice.

The spleen is a reservoir of monocytes, which can be mobilized to the heart and subsequently contribute to cardiac inflammation and remodeling [93]. The percentage of splenic $CD68^+$ monocytes was 1.2-fold ($p<0.0001$) higher in CVB3-infected mice compared to uninfected control mice (**Figure 15A**), whereas the percentage of splenic $CD68^+$ monocytes was 1.1-fold ($p<0.01$) lower in colchicine-treated CVB3-infected mice versus untreated CVB3-infected mice (**Figure 15A**). $CD68^+$ cells presence in the LV was 3.2-fold ($p<0.001$) higher in CVB3-infected mice compared to uninfected control mice (**Figure 15B**). Colchicine damped the LV $CD68^+$ monocytes presence in CVB3-induced myocarditis mice, as indicated by 2.3-fold ($p<0.005$) lower $CD68^+$ cells in the LV of colchicine-treated CVB3-infected mice compared to untreated CVB3-infected mice (**Figure 15B**).

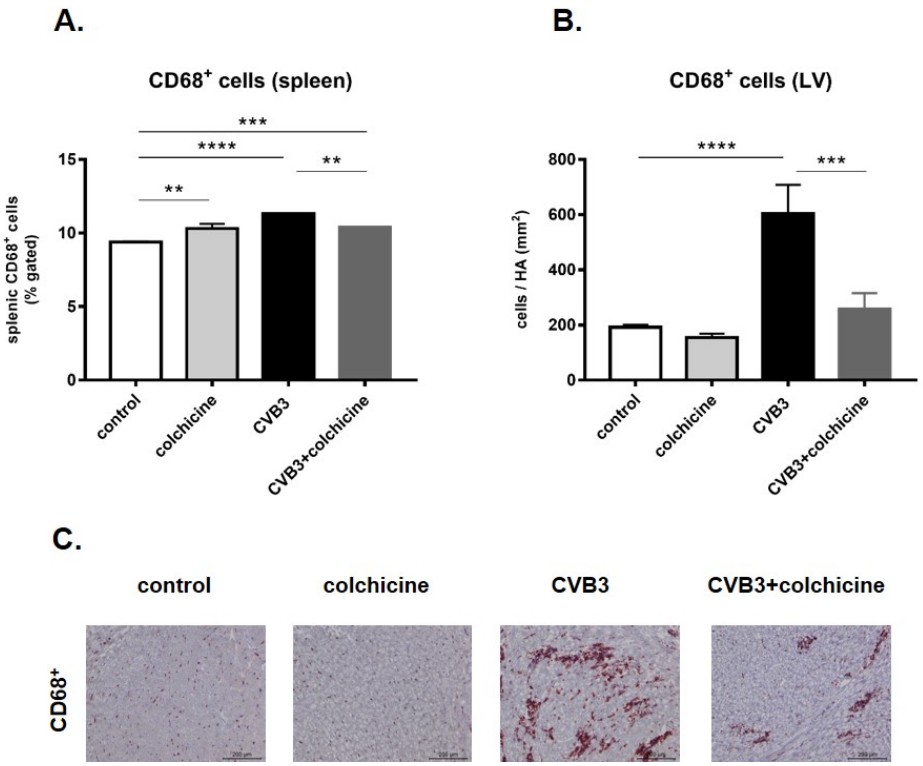

Figure 15. Colchicine decreased $CD68^+$ cells in the spleen and left ventricle of Coxsackievirus B3-infected mice. Bar graphs represent mean±SEM of **A.** the percentage of $CD68^+$ cells in the spleen and **B.** the amount of $CD68^+$ cells per heart area (HA) (mm^2) in the LV, of control, colchicine, Coxsackievirus B3-infected (CVB3) and CVB3-infected mice treated with colchicine (CVB3+colchicine) respectively. Statistical analysis was performed by One-way ANOVA. (**p<0.01, ***p<0.001, ***p<0.0001, with n=12 for control group, n=15 for colchicine and CVB3 groups, n=18 for CVB3+colchicine group). **C.** Representative images of $CD68^+$ cells in the LV of control, colchicine, CVB3 and CVB3+colchicine mice, at 100× magnification.

4.2.5.3. Impact of colchicine on Ly6C and TNF-α mRNA expression in the left ventricle of Coxsackievirus B3-induced myocarditis mice

LV mRNA expression of the inflammatory markers Ly6C and TNF-α was 3.2-fold ($p<0.0001$) and 11-fold ($p<0.0001$) higher in CVB3-infected versus control mice (**Figure 16, A-B**). Colchicine intervention lowered the mRNA expression of Ly6C and TNF-α in CVB3-infected mice as indicated by 1.4-fold ($p<0.05$) and 2.1-fold ($p<0.05$) lower LV Ly6C and TNF-α mRNA expression in CVB3+colchicine compared to CVB3-infected mice, respectively (**Figure 16, A-B**).

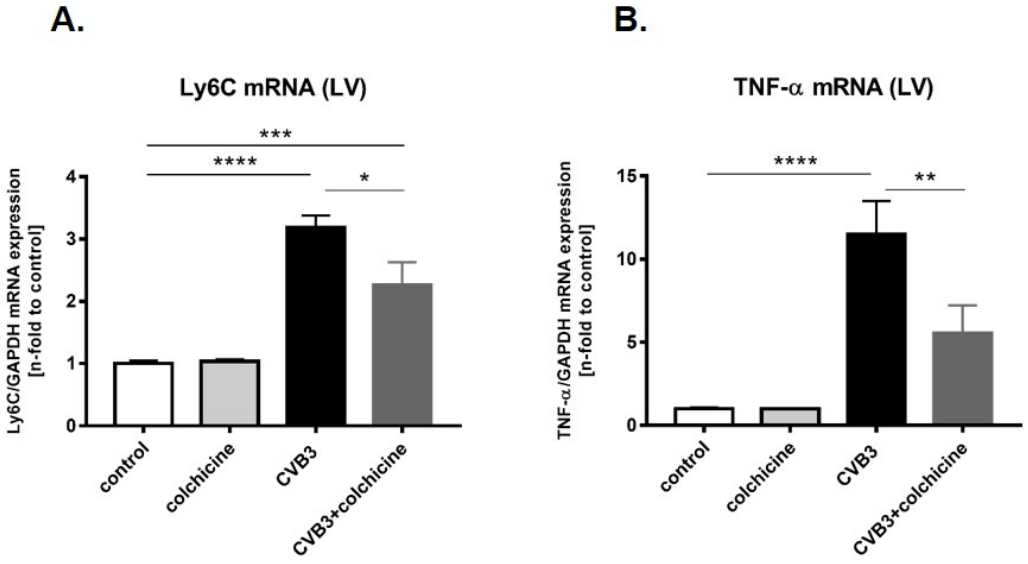

Figure 16. Colchicine reduces the left ventricular mRNA expression of inflammatory markers in Coxsackievirus B3-induced myocarditis mice. Bar graphs represent mean±SEM of LV **A.** Ly6C and **B.** TNF-α mRNA expression of control, colchicine, Coxsackievirus B3-infected (CVB3) and CVB3-infected mice treated with colchicine (CVB3+colchicine), respectively. Statistical analysis was performed by One-way ANOVA. (*$p<0.05$, **$p<0.01$, ***$p<0.001$, ****$p<0.0001$, with n=12 for control and CVB3 groups, n=15 for colchicine group, n=14 for CVB3+colchicine group).

4.2.5.4. Impact of colchicine on Ly6C^{high}, Ly6C^{middle} and Ly6C^{low} cells in the spleen of Coxsackievirus B3-induced myocarditis mice

Monocytes are a heterogeneous multifunctional cellular population, of which CD115^{+}CD11b^{+}Ly6C^{high} CCR2^{high}Cx3Cr1^{low} cells (Ly6C^{high}) and CD115^{+}CD11b^{+} Ly6C^{middle}CCR2^{high}Cx3Cr1^{low} cells (Ly6C^{middle}) infiltrate to sites of inflammation in response to chemokine signals and differentiate into inflammatory M1 macrophages, secreting

pro-inflammatory cytokines whereas $CD115^{+}$ $CD11b^{+}Ly6C^{low}$ $CCR2^{low}Cx3Cr1^{high}$ monocytes ($Ly6C^{low}$) are recruited to the inflamed tissue and are more likely to differentiate into M2 macrophages, secreting anti-inflammatory cytokines [88].

The percentage of splenic $Ly6C^{high}$ and $Ly6C^{middle}$ cells was 1.4-fold ($p<0.001$) and 1.4-fold ($p<0.001$) higher in CVB3-infected mice compared to uninfected control mice, respectively (**Figure 17, A-B**). In contrast, the percentage of anti-inflammatory $Ly6C^{low}$ cells was 2.3-fold ($p<0.0001$) lower in CVB3-infected mice than in uninfected control mice (**Figure 17C**). The percentage of $Ly6C^{low}$ monocytes was 1.1-fold ($p<0.01$) higher in colchicine-treated CVB3-infected mice than in untreated CVB3-infected mice (**Figure 17C**).

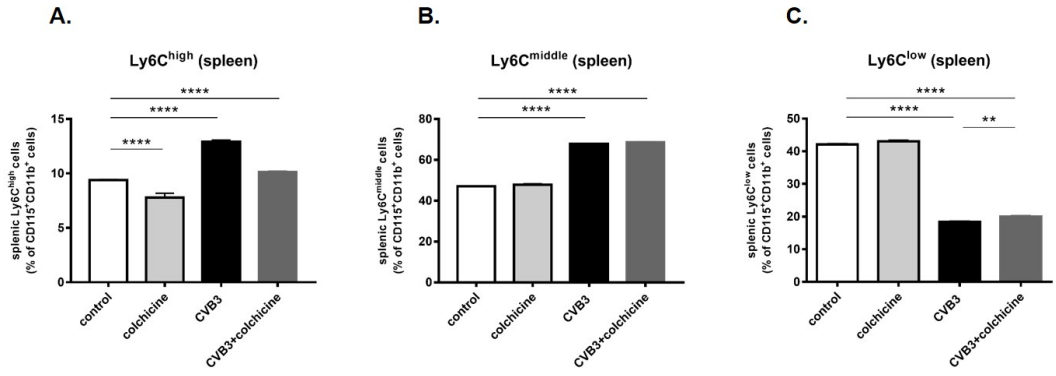

Figure 17. Colchicine modulates the percentage of pro-inflammatory $Ly6C^{high}$ and $Ly6C^{middle}$, and anti-inflammatory $Ly6C^{low}$ cells in the spleen of Coxsackievirus B3-induced myocarditis mice. Bar graphs represent the mean±SEM of splenic **A.** $Ly6C^{high}$, **B.** $Ly6C^{middle}$, and **C.** $Ly6C^{low}$ monocytes as a % of CD115+CD11b+ cells, of control, colchicine, Coxsackievirus B3-infected (CVB3) and CVB3-infected mice treated with colchicine (CVB3+colchicine), respectively. Statistical analysis was performed by One-way ANOVA. (**p<0.01, ****p<0.0001, with n=6 for control, colchicine, CVB3, and CVB3+colchicine groups).

4.2.5.5. Impact of colchicine on the NLRP3 inflammasome in the left ventricle of Coxsackievirus B3-induced myocarditis mice

The NLRP3 inflammasome has been shown to play an important role in the pathogenesis of CVB3-induced myocarditis [94]. LV mRNA expression of the components of the NLRP3 inflammasome, LV NLRP3 and caspase 1 mRNA expression was 4.6-fold ($p<0.01$) and 3.1-fold ($p<0.0001$) higher in CVB3-infected mice compared to uninfected control mice, respectively (**Figure 18, A-C**). Colchicine did not affect LV NLRP3 and ASC mRNA expression in CVB3-infected mice (**Figure 18, A-B**), neither did it reduce LV ASC protein expression (**Figure**

18D). In contrast, 1.6-fold ($p<0.05$) lower LV caspase 1 mRNA expression was found in colchicine-treated CVB3-infected mice compared to untreated CVB3-infected mice (**Figure 18C)**.

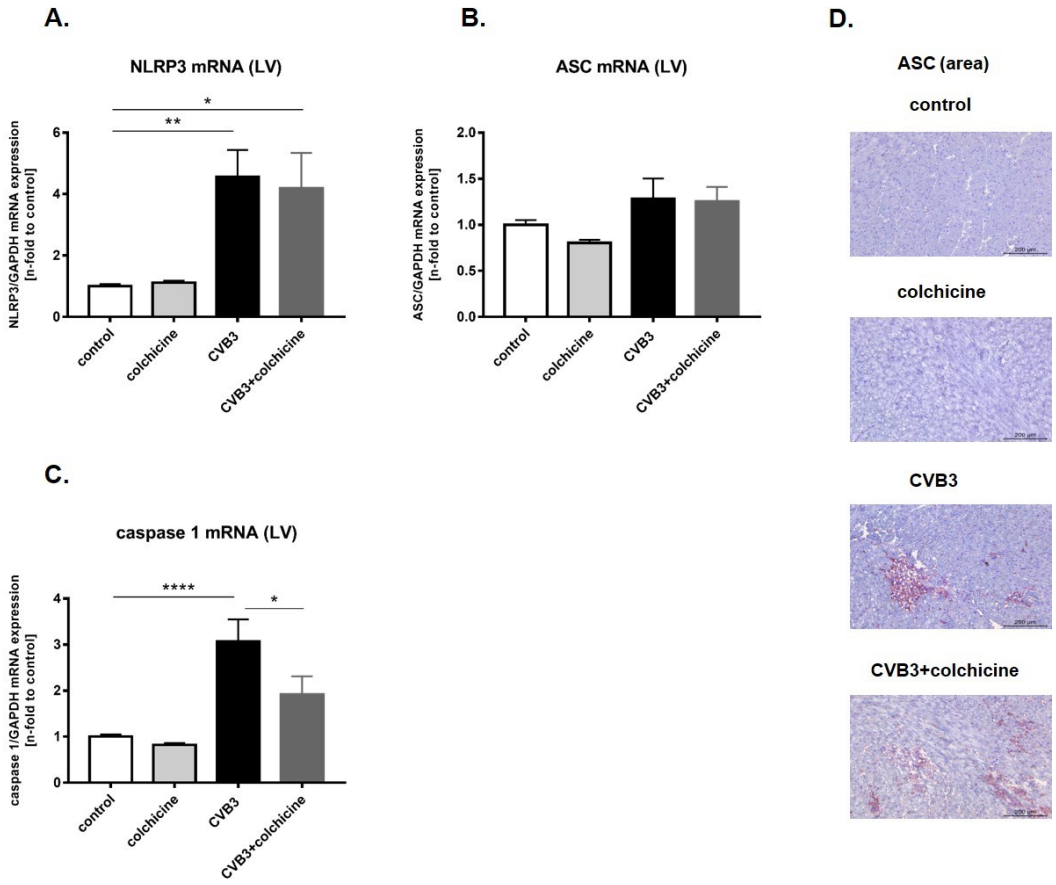

Figure 18. Colchicine affects the expression of components of the NLRP3 inflammasome in the left ventricle of Coxsackievirus B3-induced myocarditis mice. Bar graphs represent mean±SEM of LV **A.** NLRP3, **B.** ASC, and **C.** caspase 1 mRNA expression in control, colchicine, CVB3 and CVB3+colchicine mice. Statistical analysis was performed by One-way ANOVA. (*p< 0.05, **p<0.01, ****p<0.0001, with n=12 for control and CVB3 groups, n=15 for colchicine group, n=14 for CVB3+colchicine group). **D.** Representative images of ASC-stained LV sections of control, colchicine, CVB3 and CVB3+colchicine mice, at 100× magnification.

Next, the impact of colchicine on the % of ASC-, caspase 1-, and IL-1β-expressing cells in the heart was analyzed via flow cytometry. ASC-, caspase 1-, and IL-1β-expressing cells were 1.8-fold ($p<0.0001$), 2.4-fold ($p<0.0001$), and 1.2-fold ($p<0.0001$) higher in CVB3-infected mice than in uninfected control mice, respectively (**Figure 19, A-C)**. Colchicine decreased the % of ASC-, caspase 1-, and IL-1β-expressing cells in the heart of CVB3-infected mice, as indicated by 1.4-fold ($p<0.0001$), 1.6-fold ($p<0.0001$), and 1.2-fold ($p<0.0001$) lower ASC-, caspase 1-, and

IL-1β-positive cells in CVB3+colchicine versus untreated CVB3-infected mice, respectively (**Figure 19, A-C)**.

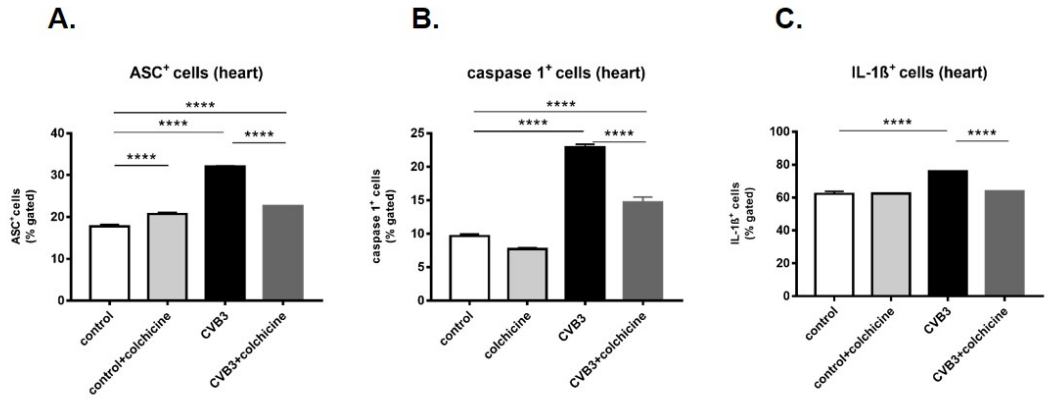

Figure 19. Colchicine reduced the % of cells expressing components of the NLRP3 inflammasome in the heart of Coxsackievirus B3-induced myocarditis mice. Bar graphs represent the mean±SEM of the percentage of **A.** ASC-, **B.** caspase 1-, and **C.** IL-1β-positive cells in the heart of control, colchicine, Coxsackievirus B3-infected (CVB3) and CVB3-infected mice treated with colchicine (CVB3+colchicine), respectively. Statistical analysis was performed by One-way ANOVA. (****p<0.0001, with n=4/group).

4.2.6. Impact of colchicine on Coxsackievirus B3 mRNA expression in the left ventricle of Coxsackievirus B3-induced myocarditis mice

To evaluate whether colchicine exerted antiviral effects in CVB3-infected mice, LV CVB3 mRNA expression was evaluated. CVB3 mRNA expression was 4.7-fold (p<0.01) lower in the LV of colchicine-treated CVB3-infected mice compared to untreated CVB3-infected mice (**Figure 20**).

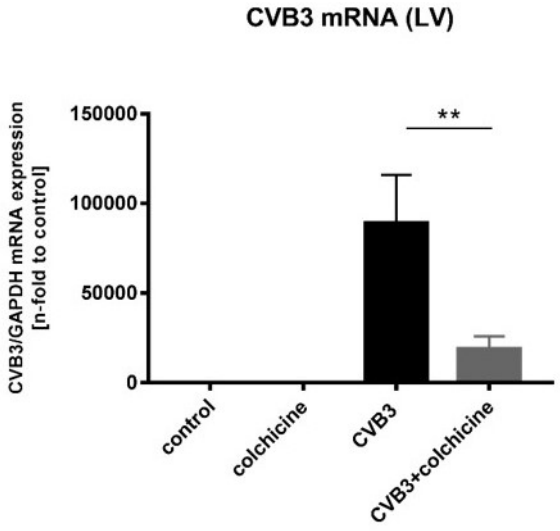

Figure 20. Impact of colchicine on left ventricular Coxsackievirus B3 mRNA expression in Coxsackievirus B3-induced myocarditis mice. Bar graph represents mean±SEM of LV Coxsackievirus B3 (CVB3) mRNA expression in control, colchicine, CVB3 and CVB3+colchicine mice. Statistical analysis was performed by One-way ANOVA. (**p<0.01, with n=12 for control and CVB3 groups, n=15 for colchicine group, n=14 for CVB3+colchicine group).

5. Discussion

Myocarditis is a cardiac inflammatory disease with a high variety in clinical presentation and underlying pathogenesis. To date, it is still challenging to obtain an early accurate diagnosis, and specific treatment options are not yet available.

There is a consensus that the excess of cardiac inflammation after infection plays a crucial role in myocytes injury, which induces cardiac dysfunction. Despite the fact that colchicine, as an ancient anti-inflammatory drug, has been widely used for the treatment of gout and familial Mediterranean fever, its exact mechanism of action is still under exploration. Colchicine was first approved by the U.S. Federal Drug Administration in 2009. Since then, accumulating evidence has demonstrated that colchicine might be a potential immune system regulator in cancer as well as cardiac and dermatological diseases [95]. So far, most of the studies investigated the impact of colchicine in sterile inflammation [95], whereas only sporadic studies focused on colchicine's anti-inflammatory effect in viral peri/myocarditis [76, 83, 84].

5.1. Impact of colchicine on Coxsackievirus B3-infected HL-1 cells

In this *in vitro* study, we were able to demonstrate that CVB3 induced HL-1 cell apoptosis, which could be attenuated with colchicine. Cell apoptosis is a comprehensive result of cell damage, which might be due to a direct CVB3-mediated injury and a CVB3-induced cellular inflammatory response. CVB3 replication plays a crucial role in CVB3-induced HL-1 cell apoptosis [96]. Previous researchers have demonstrated the relevance of CAR for the internalization of CVB3 into the cell [97]. CVB3 extremely increased the % of CAR-expressing cells, which is consistent with other studies [98]. In contrast, the % of CAR-expressing cells was less in colchicine-treated compared to untreated CVB3-infected cells. The exact mechanism of how colchicine reduces CAR expression on CVB3-infected cells is still unclear. However, since CAR expression is known to be induced by inflammatory mediators [98-100], the colchicine-mediated reduction in CAR-expressing cells is suggested to be due to a decrease in CAR expression via colchicine's anti-inflammatory properties. The binding of CAR to microtubules on the one hand [101], and the colchicine-mediated disruption of microtubule polymerization on the other hand [102], further suggest a direct effect of colchicine on the cellular/structural presence of CAR (post-translational effect). Interestingly, CAR is known to play a key role in coordinating cell-cell adhesion and

leukocyte transmigration [103, 104], supporting that the colchicine-mediated reduction in CAR may further trigger the colchicine-initiated anti-inflammatory response. The decrease in CAR-expressing HL-1 cardiomyocytes further implies a lower viral uptake and consequently less CVB3-induced apoptosis. Since cardiomyocyte apoptosis in its turn is important for viral progeny, this would consequently lead to less viral infection. This is confirmed by Wang *et al.* [94]: an increase in NLRP3 inflammasome activity was observed in CVB3-infected versus non-infected HL-1 cardiomyocytes. In agreement with the ability of colchicine to reduce NLRP3 activity [102], a lower % of ASC-, caspase 1-, and IL-1β-expressing HL-1 cells was observed in colchicine CVB3-infected versus untreated CVB3-infected cells. IL-1β inversely correlates with antiviral IFN-β [73], suggesting that the colchicine-mediated decrease in NLRP3 activity may further decrease CVB3 and subsequent apoptosis.

The colchicine-mediated cardiomyocyte-protective effects seen in CVB3-infected HL-1 cardiomyocytes, stimulated us to further evaluate the impact of colchicine in CVB3-infected C57BL/6j myocarditis mice.

5.2. Impact of colchicine on body weight and cardiac function in Coxsackievirus B3-induced myocarditis

5.2.1. Impact of colchicine on body weight in Coxsackievirus B3-induced myocarditis

Acute body weight loss is considered as a visible primary parameter for assessing morbidity of acute myocarditis in mice. Wang *et al.* [94] demonstrated a direct correlation between cardiac IL-1β levels and loss in body weight. In our study, CVB3-infected mice displayed a significant lower body weight compared to control mice. However, in contrast to Wang *et al.* [94] who observed an increase in body weight following treatment with the caspase-1 inhibitor Ac-YVAD-CHO to block inflammasome activation, colchicine could not overcome the loss in body weight. This discrepancy may partly be explained by the differences in mouse background between the study of Wang *et al.* [94] and our study.

5.2.2. Impact of colchicine on cardiac function in Coxsackievirus B3-induced myocarditis

LV hemodynamic function is the most important parameter for indicating the hazardous effect of viral myocarditis. There are several mechanisms underlying impaired cardiac function in

CVB3-induced myocarditis: 1) direct virus-induced myocardial injury involving inhibition of host cell proteins synthesis, energy consumption for viral replication and myocytes lysis induced by virus release; 2) inflammation-induced myocardial impairment due to inflammatory cell infiltration and associated inflammatory mediators (cytokines, chemokines, and antibodies); and 3) the deposition of collagen and heart remodeling, leading to impaired systolic and diastolic function [105]. As instantaneous heart function is affected by many factors and regulated by both nervous and humoral regulation, the immediate and accurate measurement of cardiac function is still challenging. Currently, magnetic resonance image (MRI), echocardiography, and left ventriculography are performed to measure cardiac function, but none of them can present the volume and pressure of the ventricle synchronically. In contrast, PV-loop measurements via conductance catheter are a competitive approach for the instant hemodynamic presentation of both volume and pressure. LVP_{max}, dP/dt_{max} and EF are three typical parameters to represent cardiac systolic function, whereas dP/dt_{min} and Tau are two main parameters to indicate the diastolic state of the heart [106]. Cardiac diastolic dysfunction has been described as an early stage of global heart pump dysfunction in viral myocarditis [107]. Related to cardiac function, it has been demonstrated that colchicine can improve cardiac function in an experimental murine myocardial infarction model via inhibition of NLRP3 inflammasome activation and downregulation of the inflammatory response [108]. In agreement, we showed that CVB3-induced myocarditis deteriorated cardiac function, whereas colchicine improved systolic function (EF, CO, LVP_{max}, and dP/dt_{max}), and diastolic function (dP/dt_{min} and Tau) in CVB3-induced myocarditis. The colchicine-mediated improvement in global cardiac function in CVB3-induced myocarditis might be explained by the inhibition of inflammatory cell infiltration, decrease in NLRP3 inflammasome activity and the reduction in cardiomyocyte apoptosis following the *in vitro* findings. Potential mechanisms explaining the improvement in cardiac function following colchicine treatment in CVB3 myocarditis mice will be described in the following.

5.3. Impact of colchicine on cardiac fibrosis in Coxsackievirus B3-induced myocarditis

Fibrosis is characterized by excessive deposition of extracellular matrix (ECM) proteins in the myocardium. Beyond the increase in quantity of the main collagen fibers, collagen 1 (col1) and

collagen 3 (col3), fibrosis is further characterized by an increase in crosslinking of collagen fibers. Fibrosis distorts the architecture of the myocardium, and promotes the progression of cardiac stiffness, which leads to diastolic and systolic dysfunction [109]. Myocardial fibrosis is a common remodeling process following inflammatory injury after viral infection. There are intricate cellular and molecular mechanisms that involve activation of fibroblasts and subsequent pathologic remodeling. Pro-fibrotic factors, including cytokines, chemokines, growth factors, and reactive oxygen species (ROS), activate fibroblasts and alter the deposition of the ECM. This causes an imbalance in the composition and homeostasis of the interstitial matrix leading to cardiac fibrosis [110]. Inflammatory signal pathways are regarded as playing a crucial role in both regional and diffuse cardiac fibrosis [111]. As part of the inflammatory response, a large number of immune cells including macrophages, monocytes, and lymphocytes infiltrate into the inflammatory areas and release pro-inflammatory factors modulating cardiac fibrosis. Pro-inflammatory cytokines, such as TNF-α, IL-1β, and IL-6, and the pro-fibrotic factor TGF-β have been shown to induce proliferation of fibroblasts and activate the transdifferentiation of fibroblasts into myofibroblasts [111-114]. Moreover, active fibroblasts in their turn can boost the inflammatory process involving the release of chemokines and cytokines among others [111, 114].

Colchicine has been shown to reduce fibrosis in the kidney [115, 116], liver [117], and heart [118]. Various colchicine-mediated anti-fibrotic effects have been reported including inhibition of AngII-induced fibroblasts migration and suppression of Ras activation [115], and decrease in TGF-β activity, CTGF expression and Rho signaling [116].

In this study, CVB3 infection increased Col1, Col3, and LOX mRNA expression in the LV, whereas colchicine downregulated Col1 and LOX mRNA expression, supporting the anti-fibrotic effects of colchicine. In both *in vitro* and *in vivo* experiments, we demonstrated that colchicine reduces NLRP3 activity, including their reduction in the presence of IL-1β-expressing cells. With the knowledge that the NLRP3 inflammasome is a prominent regulator of fibrosis [119], we suggest that the anti-fibrotic effects seen after colchicine treatment in CVB3 mice are partly due to the decrease in NLRP3 inflammasome activity.

5.4. Impact of colchicine on cardiac inflammation and immune regulation in Coxsackievirus B3-induced myocarditis

5.4.1. Impact of colchicine on chemokines/chemokine receptor in Coxsackievirus B3-induced myocarditis

Chemokines-induced inflammatory cell mobilization and migration plays a crucial role in cardiac inflammation development [120]. Chemokines comprise a large family of proteins functionally divided into inflammatory and homeostatic chemokines. The induction of inflammatory chemokines is considered as a prominent response to cardiac injury in a variety of situations such as myocardial infarction [121]. The chemokines CCL2 and CCL7 are particularly responsible for the migration and mobilization of pro-inflammatory monocytes [121]. In this study, CVB3-induced myocarditis prominently increased LV CCL2 and CCL7 mRNA expression, and colchicine treatment had no significant effect on LV CCL2 and CCL7 mRNA expression in CVB3-infected mice. In contrast, LV mRNA expression of Cx3Cr1 was higher in colchicine-treated CVB3-infected mice than untreated CVB3-infected mice. The Cx3Cl1/Cx3Cr1 system has previously been shown to be involved in a variety of cardiac pathophysiology, including inflammatory cardiomyopathy [122]. Although the relationship between Cx3Cr1 and the inflammatory response is still debatable [92, 122], this study is consistent with our center's previous research, which demonstrated that Cx3Cr1 knockout mice aggravated CVB3-induced myocarditis, which impaired LV global function [92].

5.4.2. Impact of colchicine on monocytes/macrophages and dendritic cells in Coxsackievirus B3-induced myocarditis

Monocytes arise from hematopoietic stem cells in the bone marrow and enter into the blood as still immature cells, which are thought of as the precursors of macrophages. Monocytes are important cells of innate immunity and further participate in the immune response by presenting antigen to lymphocytes. At present, murine blood monocytes (CD68+ cells) are generally divided into three subsets: classical monocytes ($Ly6C^{++}$,$CD43^{+}$; $Ly6C^{high}$), intermediate monocytes ($Ly6C^{++}$,$CD43^{++}$; $Ly6C^{middle}$), and non-classical monocytes ($Ly6C^{+}$, $CD43^{++}$; $Ly6C^{low}$), also referred to as $Ly6C^{high}$, $Ly6C^{middle}$, and $Ly6C^{low}$ cells [123]. Classical monocytes are considered as a pro-inflammation subdivision, and non-classical monocytes have anti-inflammatory

properties [124, 125]. CD115 has been shown as an ideal mouse blood monocyte marker and over 95% of $CD115^{+}$ cells co-express $CD11b^{+}$ [126]. Furthermore, based on the chemokine receptors, $Ly6C^{high}$ express $CCR2^{high}/Cx3Cr1^{low}$, and $Ly6C^{low}$ express $CCR2^{low}/ Cx3Cr1^{high}$ [123]. In agreement with previous studies [91], CVB3 infection raised CD68+ cells and boosted the proportion of $Ly6C^{high}$ and lessened the proportion of $Ly6C^{low}$ in the spleen. In parallel, LV Ly6C and TNF-α mRNA expression and CD68+ cells presence were increased in CVB3-infected mice. Colchicine decreased the CVB3-induced splenic CD68+ cells, tended to reduce the pro-inflammatory $Ly6C^{high}$ cells, and increased anti-inflammatory splenic $Ly6C^{low}$ cells in CVB3 mice. The colchicine-mediated modulation in splenic CD68+, $Ly6C^{high}$ and $Ly6C^{low}$ cells was associated with decreased LV CD68+ cell presence and LV Ly6C and TNF-α mRNA expression in CVB3-infected mice.

Since the spleen is known as a monocyte reservoir from which monocytes can move into the heart, differentiate into macrophages and dendritic cells, and contribute to cardiac inflammation and remodeling [93], these data suggest that colchicine inhibited the infiltration of CD68+ cells and pro-inflammatory Ly6C monocytes into the heart with subsequent reduction in the secretion of the strong pro-inflammatory cytokine TNF-α in CVB3-induced myocarditis.

Paradigm-shifting studies have established that in mice the heart contains a heterogeneous population of functionally distinct macrophages: cardiac resident macrophages (CCR2- macrophages) with cardioprotective/regenerative capacity, and macrophages, which arise from recruited monocytes and participate in the initiation of inflammation (CCR2+ macrophages) [127-129]. Since CD68+ subsets have not been evaluated in detail in the heart, the specific impact of colchicine on residing macrophages and infiltrating monocytes cannot be distinguished. However, a colchicine-mediated impact on the decrease in infiltrating pro-inflammatory monocytes might be expected due to the reduction in LV TNF-α mRNA expression and IL-1β-expressing cells found in colchicine-treated CVB3-infected mice.

In parallel to the increased CD68+ cell presence, CVB3-infected mice further displayed a higher presence of CD11c+ dendritic cells than in control mice, a finding, which is in agreement with Chen *et al.* [130]. Dendritic cells present antigens on the cell surface to the T cells of the immune system and act as a messenger between the innate and the adaptive immune system. Colchicine did not reduce the infiltration of CD11c+ dendritic cells in CVB3-infected mice.

However, since microtubules are important for the stability of dendrites in dendritic cells and antigen presentation [131, 132], we cannot exclude that colchicine had an impact on the antigen presentation of CD11c+ cells.

5.4.3. Impact of colchicine on T lymphocytes in Coxsackievirus B3-induced myocarditis

T lymphocytes play a crucial role in the pathogenesis of myocarditis, which follows from an early study reporting that CD8 and CD4 depletion improved the LV function in CVB3-induced myocarditis [133]. It has been well demonstrated that the T cell-mediated viral elimination is accompanied by myocardial damage [18]. Experiments further focused on subsets of T helper cells illustrated that Th1 responses protect against CVB3-induced myocarditis by inhibiting Th2 responses and viral replication in the heart, whereas a Th2 and Th17 response aggravates CVB3-induced acute myocarditis leading to dilated cardiomyopathy or heart failure [38]. In contrast, T regulatory cells (Treg) exert cardioprotective effects in CVB3-induced [134] and autoimmune myocarditis [135]. In this study, the impact of colchicine on $CD4^+$ and $CD8^+$ T lymphocytes in CVB3-induced myocarditis was investigated. Colchicine did not reduce the infiltration of T cells in the LV compared to untreated CVB3-infected mice, suggesting that colchicine exerted its cardioprotective effects independent of alterations in cardiac CD4+ and CD8+ cell presence.

5.4.4. Impact of colchicine on the cardiac NLRP3 inflammasome in Coxsackievirus B3-induced myocarditis

The NLRP3-ASC-caspase 1 complex catalyzes pro-IL-1β to pro-inflammatory cytokine IL-1β [73]. Wang *et al*. [94] reported that both RIG-1 and NLRP3 are upregulated by murine CVB3-induced myocarditis in BALB/c mice. However, only downregulation of NLRP3, and not of RIG-1, could decrease IL-1β levels, indicating that NLRP3 but not RIG-I was implicated in CVB3-induced inflammasome activation. In frame with Wang *et al.* [94] and previous observations in the lab [119], an increase of NLRP3 inflammasome activity could be observed as indicated by the upregulated LV NLRP3, ASC, and caspase-1 (mRNA) expression and cardiac ASC-, caspase 1-, and IL-1β-expressing cells in the heart.

The inhibitory effect of colchicine on NLRP3 inflammasome formation, involving blockage of the

assembly and polymerization of microtubule, has been well described in sterile monosodium urinate crystal-induced inflammatory response [136, 137]. In our study, colchicine reduced LV caspase 1 mRNA expression and the % of cardiac ASC-, caspase 1-, and IL-1ß-expressing cells in CVB3-induced myocarditis C57BL/6j mice, findings, which are supported by our *in vitro* study. In contrast, Smilde *et al.* [138] showed that colchicine (2mg/kg, i.p.) aggravated CVB3-induced myocarditis in CH3 mice leading to severe illness and mortality on the third day after infection. Colchicine decreased macrophages infiltration in the heart as well as in the spleen and pancreas, but increased neutrophils migration into multiple organs, particularly, in the pancreas. Beyond our study, using the same dose but another administration route (oral gavage), other studies also using the same or even higher concentrations (10mg/kg BW) did not report such a high mortality and severe histologic injury [139, 140]. These variations in colchicine responsiveness might be explained by the differences in mouse background since both CVB3 infection and colchicine can induce acute pancreatitis depending on the mouse background [140, 141].

Recent findings from Wang *et al.* [142] further illustrated that NLRP3 deficiency exacerbates enterovirus infection in mice. NLRP3 knockout mice exhibited increased myocardial and pancreatic damage, as well as markedly impaired cardiac function compared to nontransgenic C57BL/6j control mice. In addition, Wang *et al.* demonstrated that CVB3 inactivates the NLRP3 inflammasome by degrading NLRP3 and its upstream serine/threonine-protein kinase receptor-interacting protein 1/3 via the proteolytic activity of virus-encoded proteinases. The authors therefore concluded that NLRP3 is significant in host antiviral immunity against CVB3 infection and the mechanisms by which CVB3 has evolved to counteract the host defense response. The discrepancies in NLRP3 observations between the study of Wang *et al.* [142] and our findings might be explained by the higher dose (*in vivo*: $5x10^5$ p.f.u., versus our experiments 10^5 p.f.u., and *in vitro* m.o.i 10, versus m.o.i. 2) and the younger age of mice used (6w versus 8w). Nevertheless, these discrepancies indicate the complex activation and impact of the NLRP3 inflammasome under CVB3 myocarditis and point out the danger for extrapolation of our positive findings. As long as these differences are not clarified, the use of colchicine should be limited to non-viral induced myocarditis.

5.5. Impact of colchicine on cardiac Coxsackievirus B3 expression in Coxsackievirus

B3-induced myocarditis

Colchicine reduced CVB3 mRNA expression in the LV of CVB3-induced myocarditis mice. The relevance of CAR for CVB3 uptake in cardiomyocytes [97, 143, 144] and the importance of apoptosis for viral progeny on the one hand, and our *in vitro* findings showing that colchicine attenuated CAR expression and lessened cells apoptosis in CVB3-infected HL-1 cardiomyocytes on the other, support this finding. Since IL-1β inversely correlates with antiviral IFN-β [73], the lower levels of IL-1β-expressing cells in hearts of CVB3+colchicine versus CVB3 mice suggest that the decreased LV CVB3 mRNA expression might be partly due to increased levels in antiviral IFN-β. In frame with the lower apoptosis found in colchicine-treated versus untreated CVB3-infected HL-1 cells, LV mRNA expression of TNF-α, known to have pro-apoptotic effects [145] was decreased in the LV of CVB3+colchicine compared to CVB3 mice. Finally, since the spleen is a target organ of CVB3 [146], and cardiac infiltration of CD68+ cells is less pronounced in CVB3+colchicine versus CVB3 mice, the reduced cardiac CVB3 copy number found after colchicine treatment in CVB3 mice can partly be explained via modulation of the cardiosplenic axis.

5.6. Limitations and outlook

According to our *in vitro* and *in vivo* data, colchicine had protective effects on CVB3-induced myocarditis. One of its main mechanisms includes the inhibition of the release of the pro-inflammatory cytokines IL-1β and IL-18 by reducing the formation of the NLRP3 inflammasome. Despite the positive evaluation of colchicine application in this experimental model of CVB3-induced myocarditis, further investigations are still necessary to understand other colchicine-mediated anti-inflammatory effects, beyond its impact on the NLRP3 inflammasome, including its impact on the migration of immune cells. In this study, we used C57BL6/j inbred mice for setting up CVB3-induced acute myocarditis. Following the accumulated evidence, the mouse strain and its associated immune status, has its specific disposition to CVB3 or colchicine [138, 142], limiting a general interpretation of our positive results. Particularly, due to differences in responsiveness towards colchicine and CVB3 involving the pancreas [138, 142, 147], further evaluation of the pancreas is necessary. The intriguing impact of colchicine on CAR regulation found in HL-1 cells should be further evaluated in the *in vivo* setting. Finally,

open-chest PV loop measurements can only be performed a short time before euthanasia, which limits repeated PV-loop measurements at multiple time points for confirming global heart function. Echocardiography, allowing non-invasive measurements at different timepoints should ideally still be performed.

References

1. Caforio AL, Pankuweit S, Arbustini E, Basso C, Gimeno-Blanes J, Felix SB, Fu M, Helio T, Heymans S, Jahns R, Klingel K, Linhart A, Maisch B, McKenna W, Mogensen J, Pinto YM, Ristic A, Schultheiss HP, Seggewiss H, Tavazzi L, Thiene G, Yilmaz A, Charron P, Elliott PM. Current state of knowledge on aetiology, diagnosis, management, and therapy of myocarditis: a position statement of the European Society of Cardiology Working Group on Myocardial and Pericardial Diseases. European heart journal. 2013;34(33):2636-48, 48a-48d.
2. Mason JW. Techniques for right and left ventricular endomyocardial biopsy. The American journal of cardiology. 1978;41(5):887-92.
3. Report of the WHO/ISFC task force on the definition and classification of cardiomyopathies. British heart journal. 1980;44(6):672-3.
4. Aretz HT, Billingham ME, Edwards WD, Factor SM, Fallon JT, Fenoglio JJ, Jr., Olsen EG, Schoen FJ. Myocarditis. A histopathologic definition and classification. The American journal of cardiovascular pathology. 1987;1(1):3-14.
5. Baughman KL. Diagnosis of Myocarditis: Death of Dallas Criteria. Circulation. 2006;113(4):593-5.
6. Karjalainen J, Heikkila J, Nieminen MS, Jalanko H, Kleemola M, Lapinleimu K, Sahi T. Etiology of mild acute infectious myocarditis. Relation to clinical features. Acta medica Scandinavica. 1983;213(1):65-73.
7. Karjalainen J, Heikkila J. Incidence of three presentations of acute myocarditis in young men in military service. A 20-year experience. European heart journal. 1999;20(15):1120-5.
8. Dominguez F, Kuhl U, Pieske B, Garcia-Pavia P, Tschope C. Update on Myocarditis and Inflammatory Cardiomyopathy: Reemergence of Endomyocardial Biopsy. Revista espanola de cardiologia (English ed). 2016;69(2):178-87.
9. Baboonian C, Davies MJ, Booth JC, McKenna WJ. Coxsackie B viruses and human heart disease. Current topics in microbiology and immunology. 1997;223:31-52.
10. Bowles NE, Ni J, Kearney DL, Pauschinger M, Schultheiss HP, McCarthy R, Hare J, Bricker JT, Bowles KR, Towbin JA. Detection of viruses in myocardial tissues by polymerase chain reaction. evidence of adenovirus as a common cause of myocarditis in children and adults. Journal of the American College of Cardiology. 2003;42(3):466-72.
11. Bock CT, Klingel K, Kandolf R. Human parvovirus B19-associated myocarditis. The New England journal of medicine. 2010;362(13):1248-9.
12. Yoshikawa T, Ihira M, Suzuki K, Suga S, Kito H, Iwasaki T, Kurata T, Tanaka T, Saito Y, Asano Y. Fatal acute myocarditis in an infant with human herpesvirus 6 infection. Journal of clinical pathology. 2001;54(10):792-5.
13. Ishikawa T, Zhu BL, Li DR, Zhao D, Maeda H. Epstein-Barr virus myocarditis as a cause of sudden death: two autopsy cases. International journal of legal medicine. 2005;119(4):231-5.
14. Maisch B, Schonian U, Crombach M, Wendl I, Bethge C, Herzum M, Klein HH. Cytomegalovirus associated inflammatory heart muscle disease. Scandinavian journal of infectious diseases Supplementum. 1993;88:135-48.
15. Boyella V, Onyebueke I, Farraj N, Graham-Hill S, El Younis C, Bergasa NV. Prevalence of hepatitis C virus infection in patients with cardiomyopathy. Annals of hepatology. 2009;8(2):113-5.
16. Patane S, Marte F, Sturiale M, Dattilo G, Albanese A. Myocarditis and cardiomyopathy HIV associated. International journal of cardiology. 2011;146(3):e56-7.
17. Warren-Gash C, Smeeth L, Hayward AC. Influenza as a trigger for acute myocardial infarction or death from cardiovascular disease: a systematic review. The Lancet Infectious diseases. 2009;9(10):601-10.
18. Cooper LT, Jr. Myocarditis. The New England journal of medicine. 2009;360(15):1526-38.
19. Fung G, Luo H, Qiu Y, Yang D, McManus B. Myocarditis. Circulation research. 2016;118(3):496-514.
20. Kuhl U, Pauschinger M, Noutsias M, Seeberg B, Bock T, Lassner D, Poller W, Kandolf R, Schultheiss HP. High prevalence of viral genomes and multiple viral infections in the myocardium of adults with "idiopathic" left ventricular dysfunction. Circulation. 2005;111(7):887-93.

21. Yajima T, Knowlton KU. Viral myocarditis: from the perspective of the virus. Circulation. 2009;119(19):2615-24.
22. Loscalzo J. Keshan disease, selenium deficiency, and the selenoproteome. The New England journal of medicine. 2014;370(18):1756-60.
23. Felker GM HW, Hare JW, Hruban RH, Baughman KL, Kasper EK. The spectrum of dilated cardiomyopathy. The Johns Hopkins experience in 1278 patients. Medicine. 1999;78(4):270-83.
24. Alida L. P. Caforio SB, Sabino Iliceto. Dilated cardiomyopathy (DCM) and myocarditis: Classification, clinical and autoimmune features. Applied Cardiopulmonary Pathophysiology. 2012;16:82-9.
25. Gore I, Saphir O. Myocarditis; a classification of 1402 cases. American heart journal. 1947;34(6):827-30.
26. Basso C, Calabrese F, Corrado D, Thiene G. Postmortem diagnosis in sudden cardiac death victims: macroscopic, microscopic and molecular findings. Cardiovascular research. 2001;50(2):290-300.
27. Li HS, Ligons DL, Rose NR. Genetic complexity of autoimmune myocarditis. Autoimmunity reviews. 2008;7(3):168-73.
28. Gebhard JR, Perry CM, Harkins S, Lane T, Mena I, Asensio VC, Campbell IL, Whitton JL. Coxsackievirus B3-induced myocarditis: perforin exacerbates disease, but plays no detectable role in virus clearance. The American journal of pathology. 1998;153(2):417-28.
29. Woodruff JF, Woodruff JJ. Involvement of T lymphocytes in the pathogenesis of coxsackie virus B3 heart disease. Journal of immunology (Baltimore, Md : 1950). 1974;113(6):1726-34.
30. Gauntt C, Huber S. Coxsackievirus experimental heart diseases. Frontiers in bioscience : a journal and virtual library. 2003;8:e23-35.
31. Fairweather D, Kaya Z, Shellam GR, Lawson CM, Rose NR. From infection to autoimmunity. Journal of autoimmunity. 2001;16(3):175-86.
32. Kishimoto C, Takamatsu N, Ochiai H, Kuribayashi K. Nucleotide differences of coxsackievirus B3 and chronic myocarditis. Heart and vessels. 2015;30(1):126-35.
33. Guo Y, Wu W, Cen Z, Li X, Kong Q, Zhou Q. IL-22-producing Th22 cells play a protective role in CVB3-induced chronic myocarditis and dilated cardiomyopathy by inhibiting myocardial fibrosis. Virology journal. 2014;11:230.
34. Gluck B, Schmidtke M, Merkle I, Stelzner A, Gemsa D. Persistent expression of cytokines in the chronic stage of CVB3-induced myocarditis in NMRI mice. Journal of molecular and cellular cardiology. 2001;33(9):1615-26.
35. Chow LH, Gauntt CJ, McManus BM. Differential effects of myocarditic variants of Coxsackievirus B3 in inbred mice. A pathologic characterization of heart tissue damage. Laboratory investigation; a journal of technical methods and pathology. 1991;64(1):55-64.
36. Garmaroudi FS, Marchant D, Hendry R, Luo H, Yang D, Ye X, Shi J, McManus BM. Coxsackievirus B3 replication and pathogenesis. Future microbiology. 2015;10(4):629-53.
37. Fairweather D, Cooper LT, Jr., Blauwet LA. Sex and gender differences in myocarditis and dilated cardiomyopathy. Current problems in cardiology. 2013;38(1):7-46.
38. Fairweather D, Stafford KA, Sung YK. Update on coxsackievirus B3 myocarditis. Current opinion in rheumatology. 2012;24(4):401-7.
39. Aly M, Wiltshire S, Chahrour G, Osti JC, Vidal SM. Complex genetic control of host susceptibility to coxsackievirus B3-induced myocarditis. Genes and immunity. 2007;8(3):193-204.
40. Badorff C, Lee GH, Lamphear BJ, Martone ME, Campbell KP, Rhoads RE, Knowlton KU. Enteroviral protease 2A cleaves dystrophin: evidence of cytoskeletal disruption in an acquired cardiomyopathy. Nature medicine. 1999;5(3):320-6.
41. Bergelson JM, Cunningham JA, Droguett G, Kurt-Jones EA, Krithivas A, Hong JS, Horwitz MS, Crowell RL, Finberg RW. Isolation of a common receptor for Coxsackie B viruses and adenoviruses 2 and 5. Science (New York, NY). 1997;275(5304):1320-3.

42. Akira S, Takeda K, Kaisho T. Toll-like receptors: critical proteins linking innate and acquired immunity. Nature immunology. 2001;2(8):675-80.
43. Huang CH, Vallejo JG, Kollias G, Mann DL. Role of the innate immune system in acute viral myocarditis. Basic research in cardiology. 2009;104(3):228-37.
44. Karupiah G, Xie QW, Buller RM, Nathan C, Duarte C, MacMicking JD. Inhibition of viral replication by interferon-gamma-induced nitric oxide synthase. Science (New York, NY). 1993;261(5127):1445-8.
45. Dalldorf G, Sickles GM. An Unidentified, Filtrable Agent Isolated From the Feces of Children With Paralysis. Science (New York, NY). 1948;108(2794):61-2.
46. Shaw CA, Holland PC, Sinnreich M, Allen C, Sollerbrant K, Karpati G, Nalbantoglu J. Isoform-specific expression of the Coxsackie and adenovirus receptor (CAR) in neuromuscular junction and cardiac intercalated discs. BMC cell biology. 2004;5(1):42.
47. Zimmermann A, Gerber H, Nussenzweig V, Isliker H. Decay-accelerating factor in the cardiomyocytes of normal individuals and patients with myocardial infarction. Virchows Archiv A, Pathological anatomy and histopathology. 1990;417(4):299-304.
48. Karnauchow TM, Tolson DL, Harrison BA, Altman E, Lublin DM, Dimock K. The HeLa cell receptor for enterovirus 70 is decay-accelerating factor (CD55). Journal of virology. 1996;70(8):5143-52.
49. Cheung PK, Yuan J, Zhang HM, Chau D, Yanagawa B, Suarez A, McManus B, Yang D. Specific interactions of mouse organ proteins with the 5'untranslated region of coxsackievirus B3: potential determinants of viral tissue tropism. Journal of medical virology. 2005;77(3):414-24.
50. Harvala H, Kalimo H, Bergelson J, Stanway G, Hyypia T. Tissue tropism of recombinant coxsackieviruses in an adult mouse model. The Journal of general virology. 2005;86(Pt 7):1897-907.
51. Anderson DR, Wilson JE, Carthy CM, Yang D, Kandolf R, McManus BM. Direct interactions of coxsackievirus B3 with immune cells in the splenic compartment of mice susceptible or resistant to myocarditis. Journal of virology. 1996;70(7):4632-45.
52. Mena I, Perry CM, Harkins S, Rodriguez F, Gebhard J, Whitton JL. The role of B lymphocytes in coxsackievirus B3 infection. The American journal of pathology. 1999;155(4):1205-15.
53. Eriksson U, Penninger JM. Autoimmune heart failure: new understandings of pathogenesis. The international journal of biochemistry & cell biology. 2005;37(1):27-32.
54. Ehrenfeld E. Poliovirus-induced inhibition of host-cell protein synthesis. Cell. 1982;28(3):435-6.
55. Huber SA, Gauntt CJ, Sakkinen P. Enteroviruses and myocarditis: viral pathogenesis through replication, cytokine induction, and immunopathogenicity. Advances in virus research. 1998;51:35-80.
56. Takeuchi O, Akira S. Pattern recognition receptors and inflammation. Cell. 2010;140(6):805-20.
57. Sangiuliano B, Perez NM, Moreira DF, Belizario JE. Cell death-associated molecular-pattern molecules: inflammatory signaling and control. Mediators of inflammation. 2014;2014:821043.
58. Qian qian FW, Fei Xiong, Sidong Xiong, Wei Xu. Dynamic expression profiles of PRRs following Coxsackievirus B3 infection during acute viral myocarditis. exp clin cardiol. 2014;20(6):3953-71.
59. Kawai T, Akira S. Antiviral signaling through pattern recognition receptors. Journal of biochemistry. 2007;141(2):137-45.
60. Lundgren M, Darnerud PO, Blomberg J, Friman G, Ilback NG. Sequential changes in serum cytokines reflect viral RNA kinetics in target organs of a coxsackievirus B infection in mice. Journal of clinical immunology. 2009;29(5):611-9.
61. Tschope C, Muller I, Xia Y, Savvatis K, Pappritz K, Pinkert S, Lassner D, Heimesaat MM, Spillmann F, Miteva K, Bereswill S, Schultheiss HP, Fechner H, Pieske B, Kuhl U, Van Linthout S. NOD2 (Nucleotide-Binding Oligomerization Domain 2) Is a Major Pathogenic Mediator of Coxsackievirus B3-Induced Myocarditis. Circulation Heart failure.

2017;10(9).
62. Latz E, Xiao TS, Stutz A. Activation and regulation of the inflammasomes. Nature reviews Immunology. 2013;13(6):397-411.
63. Ting JP, Lovering RC, Alnemri ES, Bertin J, Boss JM, Davis BK, Flavell RA, Girardin SE, Godzik A, Harton JA, Hoffman HM, Hugot JP, Inohara N, Mackenzie A, Maltais LJ, Nunez G, Ogura Y, Otten LA, Philpott D, Reed JC, Reith W, Schreiber S, Steimle V, Ward PA. The NLR gene family: a standard nomenclature. Immunity. 2008;28(3):285-7.
64. Dinarello CA. Immunological and inflammatory functions of the interleukin-1 family. Annual review of immunology. 2009;27:519-50.
65. Bauernfeind FG, Horvath G, Stutz A, Alnemri ES, MacDonald K, Speert D, Fernandes-Alnemri T, Wu J, Monks BG, Fitzgerald KA, Hornung V, Latz E. Cutting edge: NF-kappaB activating pattern recognition and cytokine receptors license NLRP3 inflammasome activation by regulating NLRP3 expression. Journal of immunology (Baltimore, Md : 1950). 2009;183(2):787-91.
66. Franchi L, Eigenbrod T, Nunez G. Cutting edge: TNF-alpha mediates sensitization to ATP and silica via the NLRP3 inflammasome in the absence of microbial stimulation. Journal of immunology (Baltimore, Md : 1950). 2009;183(2):792-6.
67. Py BF, Kim MS, Vakifahmetoglu-Norberg H, Yuan J. Deubiquitination of NLRP3 by BRCC3 critically regulates inflammasome activity. Molecular cell. 2013;49(2):331-8.
68. Mayor A, Martinon F, De Smedt T, Petrilli V, Tschopp J. A crucial function of SGT1 and HSP90 in inflammasome activity links mammalian and plant innate immune responses. Nature immunology. 2007;8(5):497-503.
69. Petrilli V, Papin S, Dostert C, Mayor A, Martinon F, Tschopp J. Activation of the NALP3 inflammasome is triggered by low intracellular potassium concentration. Cell death and differentiation. 2007;14(9):1583-9.
70. Rossol M, Pierer M, Raulien N, Quandt D, Meusch U, Rothe K, Schubert K, Schoneberg T, Schaefer M, Krugel U, Smajilovic S, Brauner-Osborne H, Baerwald C, Wagner U. Extracellular Ca2+ is a danger signal activating the NLRP3 inflammasome through G protein-coupled calcium sensing receptors. Nature communications. 2012;3:1329.
71. Zhou R, Yazdi AS, Menu P, Tschopp J. A role for mitochondria in NLRP3 inflammasome activation. Nature. 2011;469(7329):221-5.
72. Toldo S, Kannan H, Bussani R, Anzini M, Sonnino C, Sinagra G, Merlo M, Mezzaroma E, De-Giorgio F, Silvestri F, Van Tassell BW, Baldi A, Abbate A. Formation of the inflammasome in acute myocarditis. International journal of cardiology. 2014;171(3):e119-21.
73. Sutterwala FS, Haasken S, Cassel SL. Mechanism of NLRP3 inflammasome activation. Annals of the New York Academy of Sciences. 2014;1319:82-95.
74. Hemkens LG, Ewald H, Gloy VL, Arpagaus A, Olu KK, Nidorf M, Glinz D, Nordmann AJ, Briel M. Cardiovascular effects and safety of long-term colchicine treatment: Cochrane review and meta-analysis. Heart (British Cardiac Society). 2016;102(8):590-6.
75. Leung YY, Yao Hui LL, Kraus VB. Colchicine--Update on mechanisms of action and therapeutic uses. Seminars in arthritis and rheumatism. 2015;45(3):341-50.
76. Cosyns B, Plein S, Nihoyanopoulos P, Smiseth O, Achenbach S, Andrade MJ, Pepi M, Ristic A, Imazio M, Paelinck B, Lancellotti P. European Association of Cardiovascular Imaging (EACVI) position paper: Multimodality imaging in pericardial disease. European heart journal cardiovascular Imaging. 2015;16(1):12-31.
77. Solomon DH, Liu CC, Kuo IH, Zak A, Kim SC. Effects of colchicine on risk of cardiovascular events and mortality among patients with gout: a cohort study using electronic medical records linked with Medicare claims. Annals of the rheumatic diseases. 2016;75(9):1674-9.
78. Imazio M, Brucato A, Ferrazzi P, Pullara A, Adler Y, Barosi A, Caforio AL, Cemin R, Chirillo F, Comoglio C, Cugola D, Cumetti D, Dyrda O, Ferrua S, Finkelstein Y, Flocco R, Gandino A, Hoit B, Innocente F, Maestroni S, Musumeci F,

Oh J, Pergolini A, Polizzi V, Ristic A, Simon C, Spodick DH, Tarzia V, Trimboli S, Valenti A, Belli R, Gaita F. Colchicine for prevention of postpericardiotomy syndrome and postoperative atrial fibrillation: the COPPS-2 randomized clinical trial. Jama. 2014;312(10):1016-23.

79. Deftereos S, Giannopoulos G, Kossyvakis C, Efremidis M, Panagopoulou V, Kaoukis A, Raisakis K, Bouras G, Angelidis C, Theodorakis A, Driva M, Doudoumis K, Pyrgakis V, Stefanadis C. Colchicine for prevention of early atrial fibrillation recurrence after pulmonary vein isolation: a randomized controlled study. Journal of the American College of Cardiology. 2012;60(18):1790-6.

80. Nuki G. Colchicine: its mechanism of action and efficacy in crystal-induced inflammation. Current rheumatology reports. 2008;10(3):218-27.

81. Weisenberg RC. Microtubule formation in vitro in solutions containing low calcium concentrations. Science (New York, NY). 1972;177(4054):1104-5.

82. Demidowich AP, Davis AI, Dedhia N, Yanovski JA. Colchicine to decrease NLRP3-activated inflammation and improve obesity-related metabolic dysregulation. Medical hypotheses. 2016;92:67-73.

83. Gultekin N, Kucukates E. Microtubule inhibition therapy by colchicine in severe myocarditis especially caused by Epstein-Barr and cytomegalovirus co-infection during a two-year period: a novel therapeutic approach. JPMA The Journal of the Pakistan Medical Association. 2014;64(12):1420-3.

84. Imazio M, Spodick DH, Brucato A, Trinchero R, Adler Y. Controversial issues in the management of pericardial diseases. Circulation. 2010;121(7):916-28.

85. Baan J, Jong TT, Kerkhof PL, Moene RJ, van Dijk AD, van der Velde ET, Koops J. Continuous stroke volume and cardiac output from intra-ventricular dimensions obtained with impedance catheter. Cardiovascular research. 1981;15(6):328-34.

86. Pacher P, Nagayama T, Mukhopadhyay P, Batkai S, Kass DA. Measurement of cardiac function using pressure-volume conductance catheter technique in mice and rats. Nature protocols. 2008;3(9):1422-34.

87. Cardiff RD, Miller CH, Munn RJ. Manual immunohistochemistry staining of mouse tissues using the avidin-biotin complex (ABC) technique. Cold Spring Harbor protocols. 2014;2014(6):659-62.

88. Yang J, Zhang L, Yu C, Yang XF, Wang H. Monocyte and macrophage differentiation: circulation inflammatory monocyte as biomarker for inflammatory diseases. Biomark Res. 2014;2(1):1.

89. Van Linthout S, Savvatis K, Miteva K, Peng J, Ringe J, Warstat K, Schmidt-Lucke C, Sittinger M, Schultheiss HP, Tschope C. Mesenchymal stem cells improve murine acute coxsackievirus B3-induced myocarditis. European heart journal. 2011;32(17):2168-78.

90. Bergelson JM. Receptors mediating adenovirus attachment and internalization. Biochem Pharmacol. 1999;57(9):975-9.

91. Miteva K, Pappritz K, El-Shafeey M, Dong F, Ringe J, Tschope C, Van Linthout S. Mesenchymal Stromal Cells Modulate Monocytes Trafficking in Coxsackievirus B3-Induced Myocarditis. Stem Cells Transl Med. 2017;6(4):1249-61.

92. Muller I, Pappritz K, Savvatis K, Puhl K, Dong F, El-Shafeey M, Hamdani N, Hamann I, Noutsias M, Infante-Duarte C, Linke WA, Van Linthout S, Tschope C. CX3CR1 knockout aggravates Coxsackievirus B3-induced myocarditis. PloS one. 2017;12(8):e0182643.

93. Ismahil MA, Hamid T, Bansal SS, Patel B, Kingery JR, Prabhu SD. Remodeling of the mononuclear phagocyte network underlies chronic inflammation and disease progression in heart failure: critical importance of the cardiosplenic axis. Circulation research. 2014;114(2):266-82.

94. Yan Wang BG, Sidong Xiong. Involvement of NLRP3 inflammasome in CVB3-induced viral myocarditis. Am J Physiol Heart Circ Physiol. 2014;307:H1438-H47.

95. Dasgeb B, Kornreich D, McGuinn K, Okon L, Brownell I, Sackett DL. Colchicine: an ancient drug with novel

applications. The British journal of dermatology. 2018;178(2):350-6.
96. Li X, Zhang J, Chen Z, Yang L, Xing X, Ma X, Yang Z. Both PI3K- and mTOR-signaling pathways take part in CVB3-induced apoptosis of Hela cells. DNA and cell biology. 2013;32(7):359-70.
97. Shi Y, Chen C, Lisewski U, Wrackmeyer U, Radke M, Westermann D, Sauter M, Tschope C, Poller W, Klingel K, Gotthardt M. Cardiac deletion of the Coxsackievirus-adenovirus receptor abolishes Coxsackievirus B3 infection and prevents myocarditis in vivo. Journal of the American College of Cardiology. 2009;53(14):1219-26.
98. Niu L, Li C, Wang Z, Xu H, An X. Effects of the MAPK pathway and the expression of CAR in a murine model of viral myocarditis. Exp Ther Med. 2017;13(1):230-4.
99. Ito M, Kodama M, Masuko M, Yamaura M, Fuse K, Uesugi Y, Hirono S, Okura Y, Kato K, Hotta Y, Honda T, Kuwano R, Aizawa Y. Expression of coxsackievirus and adenovirus receptor in hearts of rats with experimental autoimmune myocarditis. Circulation research. 2000;86(3):275-80.
100. Ruppert V, Meyer T, Pankuweit S, Jonsdottir T, Maisch B. Activation of STAT1 transcription factor precedes up-regulation of coxsackievirus-adenovirus receptor during viral myocarditis. Cardiovasc Pathol. 2008;17(2):81-92.
101. Fok PT, Huang KC, Holland PC, Nalbantoglu J. The Coxsackie and adenovirus receptor binds microtubules and plays a role in cell migration. J Biol Chem. 2007;282(10):7512-21.
102. Imazio M. Colchicine for pericarditis. Trends Cardiovasc Med. 2015;25(2):129-36.
103. Ortiz-Zapater E, Santis G, Parsons M. CAR: A key regulator of adhesion and inflammation. The international journal of biochemistry & cell biology. 2017;89:1-5.
104. Morton PE, Hicks A, Ortiz-Zapater E, Raghavan S, Pike R, Noble A, Woodfin A, Jenkins G, Rayner E, Santis G, Parsons M. TNFalpha promotes CAR-dependent migration of leukocytes across epithelial monolayers. Scientific reports. 2016;6:26321.
105. Yu Q, Vazquez R, Zabadi S, Watson RR, Larson DF. T-lymphocytes mediate left ventricular fibrillar collagen cross-linking and diastolic dysfunction in mice. Matrix biology : journal of the International Society for Matrix Biology. 2010;29(6):511-8.
106. Nishio R, Sasayama S, Matsumori A. Left ventricular pressure-volume relationship in a murine model of congestive heart failure due to acute viral myocarditis. Journal of the American College of Cardiology. 2002;40(8):1506-14.
107. Tschope C, Bock CT, Kasner M, Noutsias M, Westermann D, Schwimmbeck PL, Pauschinger M, Poller WC, Kuhl U, Kandolf R, Schultheiss HP. High prevalence of cardiac parvovirus B19 infection in patients with isolated left ventricular diastolic dysfunction. Circulation. 2005;111(7):879-86.
108. Fujisue K, Sugamura K, Kurokawa H, Matsubara J, Ishii M, Izumiya Y, Kaikita K, Sugiyama S. Colchicine Improves Survival, Left Ventricular Remodeling, and Chronic Cardiac Function After Acute Myocardial Infarction. Circulation journal : official journal of the Japanese Circulation Society. 2017;81(8):1174-82.
109. Li L, Zhao Q, Kong W. Extracellular matrix remodeling and cardiac fibrosis. Matrix biology : journal of the International Society for Matrix Biology. 2018.
110. Zhang N, Wei WY, Li LL, Hu C, Tang QZ. Therapeutic Potential of Polyphenols in Cardiac Fibrosis. Frontiers in pharmacology. 2018;9:122.
111. Van Linthout S, Miteva K, Tschope C. Crosstalk between fibroblasts and inflammatory cells. Cardiovascular research. 2014;102(2):258-69.
112. Christia P, Bujak M, Gonzalez-Quesada C, Chen W, Dobaczewski M, Reddy A, Frangogiannis NG. Systematic characterization of myocardial inflammation, repair, and remodeling in a mouse model of reperfused myocardial infarction. The journal of histochemistry and cytochemistry : official journal of the Histochemistry Society. 2013;61(8):555-70.
113. Dobaczewski M, Bujak M, Li N, Gonzalez-Quesada C, Mendoza LH, Wang XF, Frangogiannis NG. Smad3

signaling critically regulates fibroblast phenotype and function in healing myocardial infarction. Circulation research. 2010;107(3):418-28.
114. Pappritz K, Savvatis K, Koschel A, Miteva K, Tschope C, Van Linthout S. Cardiac (myo)fibroblasts modulate the migration of monocyte subsets. Scientific reports. 2018;8(1):5575.
115. Itano S, Satoh M, Kadoya H, Sogawa Y, Uchida A, Sasaki T, Kashihara N. Colchicine attenuates renal fibrosis in a murine unilateral ureteral obstruction model. Molecular medicine reports. 2017;15(6):4169-75.
116. Guan T, Gao B, Chen G, Chen X, Janssen M, Uttarwar L, Ingram AJ, Krepinsky JC. Colchicine attenuates renal injury in a model of hypertensive chronic kidney disease. American journal of physiology Renal physiology. 2013;305(10):F1466-76.
117. Muntoni S, Rojkind M, Muntoni S. Colchicine reduces procollagen III and increases pseudocholinesterase in chronic liver disease. World journal of gastroenterology. 2010;16(23):2889-94.
118. Akodad M, Fauconnier J, Sicard P, Huet F, Blandel F, Bourret A, de Santa Barbara P, Aguilhon S, LeGall M, Hugon G, Lacampagne A, Roubille F. Interest of colchicine in the treatment of acute myocardial infarct responsible for heart failure in a mouse model. International journal of cardiology. 2017;240:347-53.
119. Miteva K, Pappritz K, Sosnowski M, El-Shafeey M, Muller I, Dong F, Savvatis K, Ringe J, Tschope C, Van Linthout S. Mesenchymal stromal cells inhibit NLRP3 inflammasome activation in a model of Coxsackievirus B3-induced inflammatory cardiomyopathy. Scientific reports. 2018;8(1):2820.
120. Frangogiannis NG, Entman ML. Targeting the chemokines in myocardial inflammation. Circulation. 2004;110(11):1341-2.
121. Palomino DC, Marti LC. Chemokines and immunity. Einstein (Sao Paulo, Brazil). 2015;13(3):469-73.
122. Escher F, Vetter R, Kuhl U, Westermann D, Schultheiss HP, Tschope C. Fractalkine in human inflammatory cardiomyopathy. Heart (British Cardiac Society). 2011;97(9):733-9.
123. Ziegler-Heitbrock L, Ancuta P, Crowe S, Dalod M, Grau V, Hart DN, Leenen PJ, Liu YJ, MacPherson G, Randolph GJ, Scherberich J, Schmitz J, Shortman K, Sozzani S, Strobl H, Zembala M, Austyn JM, Lutz MB. Nomenclature of monocytes and dendritic cells in blood. Blood. 2010;116(16):e74-80.
124. Nahrendorf M, Pittet MJ, Swirski FK. Monocytes: protagonists of infarct inflammation and repair after myocardial infarction. Circulation. 2010;121(22):2437-45.
125. Burke B, Ahmad R, Staples KJ, Snowden R, Kadioglu A, Frankenberger M, Hume DA, Ziegler-Heitbrock L. Increased TNF expression in CD43++ murine blood monocytes. Immunology letters. 2008;118(2):142-7.
126. Breslin WL, Strohacker K, Carpenter KC, Haviland DL, McFarlin BK. Mouse blood monocytes: standardizing their identification and analysis using CD115. Journal of immunological methods. 2013;390(1-2):1-8.
127. Nahrendorf M, Swirski FK. Monocyte and macrophage heterogeneity in the heart. Circulation research. 2013;112(12):1624-33.
128. Honold L, Nahrendorf M. Resident and Monocyte-Derived Macrophages in Cardiovascular Disease. Circulation research. 2018;122(1):113-27.
129. Liao X, Shen Y, Zhang R, Sugi K, Vasudevan NT, Alaiti MA, Sweet DR, Zhou L, Qing Y, Gerson SL, Fu C, Wynshaw-Boris A, Hu R, Schwartz MA, Fujioka H, Richardson B, Cameron MJ, Hayashi H, Stamler JS, Jain MK. Distinct roles of resident and nonresident macrophages in nonischemic cardiomyopathy. Proc Natl Acad Sci U S A. 2018;115(20):E4661-E9.
130. Chen P, Chen R, Yang Y, Yu Y, Xie Y, Zou Y, Ge J, Chen H. Coxsackievirus B3 infection promotes generation of myeloid dendritic cells from bone marrow and accumulation in the myocardium. Int Immunopharmacol. 2009;9(11):1304-12.
131. Peachman KK, Rao M, Palmer DR, Zidanic M, Sun W, Alving CR, Rothwell SW. Functional microtubules are required for antigen processing by macrophages and dendritic cells. Immunology letters. 2004;95(1):13-24.

132. Swetman Andersen CA, Handley M, Pollara G, Ridley AJ, Katz DR, Chain BM. beta1-Integrins determine the dendritic morphology which enhances DC-SIGN-mediated particle capture by dendritic cells. Int Immunol. 2006;18(8):1295-303.
133. Opavsky MA, Penninger J, Aitken K, Wen WH, Dawood F, Mak T, Liu P. Susceptibility to myocarditis is dependent on the response of alphabeta T lymphocytes to coxsackieviral infection. Circulation research. 1999;85(6):551-8.
134. Pappritz K, Savvatis K, Miteva K, Kerim B, Dong F, Fechner H, Muller I, Brandt C, Lopez B, Gonzalez A, Ravassa S, Klingel K, Diez J, Reinke P, Volk HD, Van Linthout S, Tschope C. Immunomodulation by adoptive regulatory T-cell transfer improves Coxsackievirus B3-induced myocarditis. FASEB J. 2018:fj201701408R.
135. Chen P, Baldeviano GC, Ligons DL, Talor MV, Barin JG, Rose NR, Cihakova D. Susceptibility to autoimmune myocarditis is associated with intrinsic differences in CD4(+) T cells. Clinical and experimental immunology. 2012;169(2):79-88.
136. Misawa T, Takahama M, Kozaki T, Lee H, Zou J, Saitoh T, Akira S. Microtubule-driven spatial arrangement of mitochondria promotes activation of the NLRP3 inflammasome. Nature immunology. 2013;14(5):454-60.
137. Cronstein BN, Sunkureddi P. Mechanistic aspects of inflammation and clinical management of inflammation in acute gouty arthritis. Journal of clinical rheumatology : practical reports on rheumatic & musculoskeletal diseases. 2013;19(1):19-29.
138. Smilde BJ, Woudstra L, Fong Hing G, Wouters D, Zeerleder S, Murk JL, van Ham M, Heymans S, Juffermans LJ, van Rossum AC, Niessen HW, Krijnen PA, Emmens RW. Colchicine aggravates coxsackievirus B3 infection in mice. International journal of cardiology. 2016;216:58-65.
139. Craig DH, Owen CR, Conway WC, Walsh MF, Downey C, Basson MD. Colchicine inhibits pressure-induced tumor cell implantation within surgical wounds and enhances tumor-free survival in mice. The Journal of clinical investigation. 2008;118(9):3170-80.
140. Ueda T, Takeyama Y, Adachi M, Toyokawa A, Kishida S, Yamamoto M, Saitoh Y. Effect of the microtubule-disrupting drug colchicine on rat cerulein-induced pancreatitis in comparison with the microtubule stabilizer taxol. Pancreas. 1995;11(3):294-302.
141. Yanagawa B, Spiller OB, Proctor DG, Choy J, Luo H, Zhang HM, Suarez A, Yang D, McManus BM. Soluble recombinant coxsackievirus and adenovirus receptor abrogates coxsackievirus b3-mediated pancreatitis and myocarditis in mice. The Journal of infectious diseases. 2004;189(8):1431-9.
142. Wang C, Fung G, Deng H, Jagdeo J, Mohamud Y, Xue YC, Jan E, Hirota JA, Luo H. NLRP3 deficiency exacerbates enterovirus infection in mice. FASEB J. 2019;33(1):942-52.
143. Selinka HC, Wolde A, Sauter M, Kandolf R, Klingel K. Virus-receptor interactions of coxsackie B viruses and their putative influence on cardiotropism. Medical microbiology and immunology. 2004;193(2-3):127-31.
144. Huber S, Song WC, Sartini D. Decay-accelerating factor (CD55) promotes CD1d expression and Vgamma4+ T-cell activation in coxsackievirus B3-induced myocarditis. Viral immunology. 2006;19(2):156-66.
145. Kewalramani G, Puthanveetil P, Wang F, Kim MS, Deppe S, Abrahani A, Luciani DS, Johnson JD, Rodrigues B. AMP-activated protein kinase confers protection against TNF-{alpha}-induced cardiac cell death. Cardiovascular research. 2009;84(1):42-53.
146. Klingel K, Stephan S, Sauter M, Zell R, McManus BM, Bultmann B, Kandolf R. Pathogenesis of murine enterovirus myocarditis: virus dissemination and immune cell targets. Journal of virology. 1996;70(12):8888-95.
147. Ting JY. Acute pancreatitis related to therapeutic dosing with colchicine: a case report. Journal of medical case reports. 2007;1:64.

Eidesstattliche Versicherung

„Ich, Jie Lin, versichere an Eides statt durch meine eigenhändige Unterschrift, dass ich die vorgelegte Dissertation mit dem Thema: Impact of colchicine on experimental Coxsackievirus B3-induced myocarditis selbstständig und ohne nicht offengelegte Hilfe Dritter verfasst und keine anderen als die angegebenen Quellen und Hilfsmittel genutzt habe. Alle Stellen, die wörtlich oder dem Sinne nach auf Publikationen oder Vorträgen anderer Autoren beruhen, sind als solche in korrekter Zitierung (siehe „Uniform Requirements for Manuscripts (URM)“ des ICMJE -www.icmje.org) kenntlich gemacht. Die Abschnitte zu Methodik (insbesondere praktische Arbeiten, Laborbestimmungen, statistische Aufarbeitung) und Resultaten (insbesondere Abbildungen, Graphiken und Tabellen) entsprechen den URM (s.o) und werden von mir verantwortet.

Meine Anteile an etwaigen Publikationen zu dieser Dissertation entsprechen denen, die in der untenstehenden gemeinsamen Erklärung mit dem/der Betreuer/in, angegeben sind. Sämtliche Publikationen, die aus dieser Dissertation hervorgegangen sind und bei denen ich Autor bin, entsprechen den URM (s.o) und werden von mir verantwortet.

Die Bedeutung dieser eidesstattlichen Versicherung und die strafrechtlichen Folgen einer unwahren eidesstattlichen Versicherung (§156,161 des Strafgesetzbuches) sind mir bekannt und bewusst.“

Datum Unterschrift:

Curriculum Vitae

My curriculum vitae does not appear in the electronic version of my paper for reasons of data protection.

My curriculum vitae does not appear in the electronic version of my paper for reasons of data protection.

Acknowledgements

First of all, I sincerely thank my supervisor, Prof. Dr. Carsten Tschöpe for offering the precious opportunity to perform my doctoral research in his lab and for giving definite support and encouragement during the entire period of study.

I also want to express my sincere gratitude to PD Dr. Sophie Van Linthout, who led me to the scientific research field, for her insights, careful and thoughtful for a complicated issue to easy understand throughout the research, and for her critical reading and revision of my thesis.

I am very grateful to Dr. Kathleen Pappritz, Dr. Irene Müller and Muhammad El Shafeey for their great and helpful assistance in this study.

I also want to thank Kerstin Puhl, Marzena Sosnowski and Annika Koschel for their technical assistance in my work.

I would like to express my great gratitude to the China Scholarship Council (CSC) for offering the financial support of my Dr. thesis.

Finally, I would like to thank my family especially my parents, my wife and my daughter for their selfless support, love and encouragement throughout my work and life in Berlin.